Computational Statistics and Data Analysis 203 (2025) 108092

Contents lists available at ScienceDirect

Computational Statistics and Data Analysis

journal homepage: www.elsevier.com/locate/csda

A goodness-of-fit test for functional time series with applications to Ornstein-Uhlenbeck processes

J. Álvarez-Liébana [a,*], A. López-Pérez [b], W. González-Manteiga [b], M. Febrero-Bande [b]

[a] Department of Statistics and Data Science, Faculty of Statistics, Complutense University of Madrid, Spain
[b] Department of Statistics, Mathematical Analysis and Optimization, Universidade de Santiago de Compostela, Spain

ARTICLE INFO

Keywords:
Currency exchange rates
Diffusion models
Functional time series
Goodness-of-fit
Specification test
Ornstein-Uhlenbeck process

ABSTRACT

High-frequency financial data can be collected as a sequence of time-ordered curves, such as intraday prices. The Functional Data Analysis (FDA) framework offers a powerful approach to uncover information embedded in the shape of the daily paths, often unavailable from classical statistical methods. A novel goodness-of-fit test for autoregressive Hilbertian (ARH) models is introduced, imposing only the Hilbert-Schmidt condition on the autocorrelation operator. The test statistic is formulated in terms of a Cramér–von Mises norm, with calibration achieved via a wild bootstrap resampling procedure. A simulation study examines the test's finite-sample performance in terms of power and size. Furthermore, a new specification test for diffusion models, including Ornstein-Uhlenbeck processes, is proposed, illustrated with an application to intraday currency exchange rates. Specifically, a two-stage methodology is proffered: firstly, the relationship between functional samples and their lagged values is assessed using an ARH(1) model; second, under linearity, a functional F-test is conducted.

1. Introduction

Motivated by the recent availability of high-frequency data across various domains, particularly in finance, a contribution in the field of time series of functional data, with a special focus on diffusion processes, is developed. Few papers devoted to specification tests for functional time series, and it is aimed to fill that gap by pursuing two main objectives. First, an omnibus test for functional time series under a composite null hypothesis is developed, in terms of a Crámer-von Mises statistic. Second, leveraging the characterization of the Ornstein-Uhlenbeck (OU) process as an autoregressive Hilbertian (ARH) model, a novel specification test for this diffusive model is provided.

Modeling relationships between functional random variables (frv's) remains a central focus in statistical literature, where the Functional Linear Model with Functional Response (FLMFR), $\mathcal{Y} = m(\mathcal{X}) + \mathcal{E}$, with m a linear operator and $\mathcal{E}$ a functional error, is likely the best-known model. Within a Hilbertian framework, the operator m is typically assumed to be a Hilbert-Schmidt integral operator between L^2 spaces.

The GoF setup for regression models is a well-established field in which several authors have contributed, in the context of vectorial covariates and scalar response. For a comprehensive overview, see González-Manteiga and Crujeiras (2013), as well as Kim et al. (2023) for a more recent survey on functional time series. Most of these authors have developed methodologies based on

* Corresponding author.
E-mail address: javalv09@ucm.es (J. Álvarez-Liébana).

https://doi.org/10.1016/j.csda.2024.108092
Received 13 September 2023; Received in revised form 31 October 2024; Accepted 4 November 2024

Available online 5 November 2024

the integrated regression approach introduced by Stute (1997). This framework was subsequently extended to functional contexts in García-Portugués et al. (2014), Cuesta-Albertos et al. (2019) and García-Portugués et al. (2021). The methodology in the latter paper, devoted to GoF of functional linear models, is extended to core of linear models within functional time series focusing in ARH processes, where the functional regressors are represented by their own lagged values.

A crucial aspect of GoF of ARH processes is the estimation of the associated linear operator. Early results were proposed by Bosq (2000), on the estimation of ARH(1) models $\mathcal{X}_n(\cdot) = \rho\left(\mathcal{X}_{n-1}\right)(\cdot) + \mathcal{E}_n(\cdot)$, with $n \in \mathbb{Z}$ and ρ the associated operator. See, more recently, the works of Álvarez-Liébana et al. (2017) and Ruiz-Medina and Álvarez-Liébana (2019) where the authors leverage the Hilbert space structure, as well as the broader framework of Banach spaces, for functional data.

A critical aspect when working with functional time series is determining whether a single model can adequately represent the data. Horváth and Kokoszka (2012) provide a thorough introduction to GoF for functional time series, with more recent references offering additional insights. For example, Kokoszka et al. (2017) propose statistical methods to account for time-varying volatility in autocovariance estimation, which is essential for understanding temporal dependence in high-dimensional or infinite-dimensional settings, thereby improving model diagnostics in dynamic environments (see also Rice et al. 2020 on heteroscedasticity functional data). This is particularly relevant to functional time series as it enhances the ability to detect model inadequacies, providing more robust diagnostics in the complex, infinite-dimensional data typical of functional time series analysis. The GoF proposal presented aligns with developments by Kim et al. (2024), where the authors apply projection-based methods to assess whether a given functional time series is adequately modeled as white noise or fits a proposed model, using projections to simplify high-dimensional data (see also Yeh et al. 2023 on spherical projection approaches). In financial time series literature, various studies have examined model structure. Early contributions include Laukaitis and Rackauskas (2002), who analyzed functional residuals for change-point detection (see also Berkes et al., 2009). Gabrys and Kokoszka (2007) introduced tests for independence and stationarity of functional random variables (frv's) (see also Hlávka et al., 2021). Horváth et al. (2010) proposed methods evaluate whether the autocorrelation operator remains stable over time, while in Horváth et al. (2014) the stationarity of a functional time series is tested. More recently works have focused on GoF for white noise in functional time series, as in Bagchi et al. (2018) and Zhang (2016), alongside the recent review by Kim et al. (2023).

Hence, a GoF test for ARH(z) processes is provided, under the null hypothesis

$$\mathcal{H}_0: \ \mathcal{X}_n \text{ and } \left(\mathcal{X}_{n-1}, \ldots, \mathcal{X}_{n-z}\right) \text{ linearly related}, \quad (\text{i.e., } \mathcal{X}_n(t) = \sum_{r=1}^{z} \rho_r(\mathcal{X}_{n-r})(t) + \mathcal{E}_n(t)),$$

against an unspecified alternative hypothesis (omnibus test), where $\left\{\rho_r\right\}_{r=1}^{z}$ is a set of linear operators ρ_β given by $\rho_\beta(\mathcal{X})(t) = \int_0^h \beta(s,t)\mathcal{X}(s)\mathrm{d}s$, with $\int_0^h \int_0^h \beta^2(s,t)\mathrm{d}s\mathrm{d}t < \infty$ and $z \geq 1$. The methodology reinterprets an ARH(z) process as a specific case of a FLMFR and characterizes $\mathcal{H}_0$ in terms of the integral regression operator derived, projected into finite-dimensional functional directions, following the approach of García-Portugués et al. (2021). Deviations from $\mathcal{H}_0$ are quantified using a Cramér–von Mises norm, with the test statistic calibrated via wild bootstrap. The novelty of contribution is twofold: i) a new GoF test for ARH(z) processes, for any integer order $z \geq 1$; ii) a sequential procedure for determining the order of an ARH model. While no comparable method exists for the former, the latter is compared against the order detection procedure of Kokoszka and Reimherr (2013), whose approach is limited to ARH alternatives.

Given the central role of diffusion processes in finance, a framework for model specification of diffusion models from a functional perspective is also developed. In the context of GoF tests, several approaches have been proposed for univariate continuous-time models. Some methods assess the marginal density function of the process (Aït-Sahalia, 1996 and Gao and King, 2004); the transitional density (Hong and Li, 2004; Chen et al., 2008); the cumulative distribution function (Corradi and Swanson, 2005); the conditional characteristic function (Chen and Hong, 2010); or the infinitesimal operator (Song, 2011). Nonparametric techniques have also been suggested by Arapis and Gao (2006), Gao and Casas (2008) or Zheng (2009); whilst Fan and Zhang (2003), Fan et al. (2003) and Aït-Sahalia et al. (2009) proposals were based on likelihood ratio test ideas and Chen and Gao (2011) on empirical likelihood. Other approaches include stochastic processes based on the integrated volatility function, as in Dette and von (2003), Dette and Podolskij (2008) and Podolskij and Ziggel (2008), while marked empirical process-based tests have been developed by Negri and Nishiyama (2009), Monsalve-Cobis et al. (2011) and Chen et al. (2015).

In this classical context, diffusion models for financial data are commonly used at daily, weekly or monthly frequency. However, high-frequency data constitutes time series at a very fine resolution, and using daily data would imply discarding large fractions of observations. It is in this high frequency scenario where dealing with diffusion models using a functional data approach allows to model the realized daily trajectories, analyzing the patterns of the curves across the days. Since Vasicek model was used to capture the dynamics of interest rates, the OU process (Uhlenbeck and Ornstein, 1930) is one of the main diffusion models. As an alternative for multivariate settings, a novel two-stage specification test for OU processes is proposed: in the first step, it is verified whether the underlying stochastic differential equation can be characterized via ARH(1) process, based on an ARH(1) characterization; secondly, under linearity, a functional F-test is implemented.

The remainder of the article is organized as follows. Section 2 provides a brief introduction to functional data, FLMFR, and ARH(z) models. A goodness-of-fit test for the aforementioned autoregressive models is detailed in Section 3. A simulation study, which compares our findings with those presented in Kokoszka and Reimherr (2013), is undertaken in Section 3.4. Section 4 proposes a new specification test for diffusion models. The performance of this test is illustrated through an extensive simulation study. In Section 5, we address a real-data application involving daily currency exchange rate curves. Finally, Section 6 concludes the paper, with theoretical details relegated to the Supplementary Material.

2. Background: FLMFR and functional time series

Whilst Hilbert spaces are the common option, it is well worth canvassing the alternatives which could be adopted. The most general context may be given by a metric space endowed with a distance. In contrast with metric spaces, useful when no information about curves is available but rather abstract since a norm cannot be guaranteed, a Banach space $\left(\mathbb{B}, \|\cdot\|_{\mathbb{B}}\right)$ may be adopted in place, say $C([0,1])$. Unless otherwise explicitly mentioned, separable Hilbert spaces $\left(\mathbb{H}, \langle\cdot,\cdot\rangle_{\mathbb{H}}\right)$ are considered, where $\langle\cdot,\cdot\rangle_{\mathbb{H}}$ denotes an inner product. This common choice is not arbitrary since, under separability, the existence of a countable functional basis is guaranteed. In what follows, $\left\{\Psi_j\right\}_{j=1}^{\infty}$ and $\left\{\Phi_k\right\}_{k=1}^{\infty}$ are orthonormal functional bases. From separability, any $\mathcal{X} \in \mathbb{H}_1$ and $\mathcal{Y} \in \mathbb{H}_2$ can be represented as $\mathcal{X} = \sum_{j=1}^{\infty} x_j \Psi_j$ and $\mathcal{Y} = \sum_{k=1}^{\infty} y_k \Phi_k$, with $x_j = \langle \mathcal{X}, \Psi_j \rangle_{\mathbb{H}_1}$ and $y_k = \langle \mathcal{Y}, \Phi_k \rangle_{\mathbb{H}_2}$, for each $j,k \geq 1$.

Since sparsity effects usually appear, dimension reduction is essential. This sparsity can be understood in a wide sense, such as referring to the sparsity of the model (Aneiros and Vieu, 2014), the sparsity of data (Vieu, 2018) or related to the discretization grid (Yao et al., 2005). It can further be distinguished among fixed bases (e.g., B-splines), flexible but usually require a larger number of elements, and data-driven functional bases. More parsimonious representations can be achieved with the latter ones, being the most popular choice the (empirical) Functional Principal Components (FPC), given as the eigenfunctions of the empirical covariance operator. More details on the FPC analysis can be found in Shang (2014). $C_n^{\mathcal{X}} = \frac{1}{n}\sum_{i=1}^{n} \mathcal{X}_i \otimes \mathcal{X}_i$. Henceforth, for given finite cut-off levels $p,q \geq 1$, (p,q)-truncated bases expansions are defined as $\mathcal{X}^{(p)} = \sum_{j=1}^{p} x_j \Psi_j$ and $\mathcal{Y}^{(q)} = \sum_{k=1}^{q} y_k \Phi_k$, with $\left(x_1, \ldots, x_p\right) \in \mathbb{R}^p$ and $\left(y_1, \ldots, y_q\right) \in \mathbb{R}^q$, such that $C_n^{\mathcal{X}}\left(\Psi_j\right) = \lambda_j^{\Psi}\Psi_j$ and $C_n^{\mathcal{Y}}\left(\Phi_k\right) = \lambda_k^{\Phi}\Phi_k$, for each $j = 1, \ldots, p$ and $k = 1, \ldots, q$. In what follows, the mentioned classical FPC decomposition will be considered, even though dimension reduction from frequency domain perspective may be studied (see, e.g., Hörmann et al. (2015)).

2.1. The FLMFR

In the following, $\mathcal{X} \in \mathbb{H}_1 = L^2([a,b])$, $\mathcal{Y} \in \mathbb{H}_2 = L^2([c,d])$ are centered frv's, such that $\langle f, g \rangle_{L^2([a,b])} = \int_a^b f(t)g(t)\mathrm{d}t$. A functional time series will be characterized as a particular linear model, and so, the following FLMFR setting will be introduced:

$$\mathcal{Y} = m_\beta(\mathcal{X}) + \mathcal{E}, \qquad \mathrm{E}[\mathcal{E}|\mathcal{X}] = 0, \qquad m_\beta(x) = \mathrm{E}[\mathcal{Y}|\mathcal{X} = x] \text{ Hilbert-Schmidt}, \tag{1}$$

that is, m_β admits an integral representation given by a bivariate and square-integrable kernel $\beta \in \mathbb{H}_1 \otimes \mathbb{H}_2$, where $\otimes$ denotes the tensor product between Hilbert spaces. In the aftermath of the compactness, β can be decomposed as follows:

$$m_\beta(\mathcal{X})(\cdot) = \int_a^b \beta(s,\cdot)\mathcal{X}(s)\mathrm{d}s, \qquad \beta = \sum_{j=1}^{\infty}\sum_{k=1}^{\infty} \beta_{jk}\left(\Psi_j \otimes \Phi_k\right), \qquad \iint \beta^2(s,t) < \infty,$$

where $\beta_{jk} = \langle \beta, \Psi_j \otimes \Phi_k \rangle_{\mathbb{H}_1 \otimes \mathbb{H}_2}$, for each $j,k \geq 1$, and $(f \otimes g)(\cdot) = \langle f, \cdot \rangle_{\mathbb{H}_1} g$, for each $f \in \mathbb{H}_1$ and $g \in \mathbb{H}_2$. Adopting a (p,q)-truncated component-wise orthonormal expansion, projected into $\left\{\Psi_j\right\}_{j=1}^{p}$, $\left\{\Phi_k\right\}_{k=1}^{q}$ and $\left\{\Psi_j \otimes \Phi_k\right\}_{j,k=1}^{p,q}$,

$$\mathcal{Y}^{(q)} = \sum_{k=1}^{q} y_k \Phi_k, \quad y_k = \sum_{j=1}^{p}\sum_{\ell=1}^{p} b_{\ell,k} x_j \langle \Psi_j, \Psi_\ell \rangle_{\mathbb{H}_1} + e_k, \ k = 1, \ldots, q, \quad \mathcal{E}^{(q)} = \sum_{k=1}^{q} e_k \Phi_k. \tag{2}$$

Truncation parameters (p,q) might be determined following different strategies but, as it will be detailed shortly, they will be sample-based chosen in terms of the explained variance provided by (empirical) covariance operators. Now, given a centered sample $\left\{\left(\mathcal{X}_i, \mathcal{Y}_i\right)\right\}_{i=1}^{n}$, equations (1)–(2) may be expressed as:

$$\mathbf{Y}_q = \mathbf{X}_p \mathbf{B}_{p,q} + \mathbf{E}_q, \quad \mathcal{Y}_i = \langle\langle \mathcal{X}_i, \beta \rangle\rangle + \mathcal{E}_i, \quad \langle\langle \mathcal{X}, \beta \rangle\rangle(t) := \langle \mathcal{X}, \beta(\cdot,t) \rangle_{\mathbb{H}_1}, \tag{3}$$

where $\mathbf{Y}_q$ and $\mathbf{E}_q$ are the $n \times q$ matrices with the coefficients of $\left\{\mathcal{Y}_i\right\}_{i=1}^{n}$ and $\left\{\mathcal{E}_i\right\}_{i=1}^{n}$, respectively, on $\left\{\Phi_k\right\}_{k=1}^{q}$, $\mathbf{X}_p$ is the $n \times p$ matrix with the coefficients of $\left\{\mathcal{X}_i\right\}_{i=1}^{n}$ on $\left\{\Psi_j\right\}_{j=1}^{p}$ and $\mathbf{B}_{p,q}$ is the $p \times q$ matrix with the coefficients (to be estimated) of β on $\left\{\Psi_j \otimes \Phi_k\right\}_{j,k=1}^{p,q}$. Due to the regularity conferred by the Hilbert structure, since truncation parameters will be selected by a sample-based procedure in terms of variance, it is generally the case that $n \gg p$ and $n \gg q$.

From now on, the hybrid linearly-constrained FPC Regression (FPCR-L1S) estimator, recently formulated in García-Portugués et al. (2021), is considered, which is defined as follows:

$$\hat{\mathbf{Y}}_q = \widetilde{\mathbf{X}}_{\widetilde{p}} \hat{\mathbf{B}}_{\widetilde{p},q}^{(\lambda),C} = \mathbf{H}_C^{(\lambda)} \mathbf{Y}_q = \left[\widetilde{\mathbf{X}}_{\widetilde{p}}\left(\widetilde{\mathbf{X}}_{\widetilde{p}}^T \widetilde{\mathbf{X}}_{\widetilde{p}}\right)^{-1} \widetilde{\mathbf{X}}_{\widetilde{p}}^T\right] \mathbf{Y}_q, \quad \hat{\mathbf{B}}_{\widetilde{p},q}^{(\lambda),C} = \left(\widetilde{\mathbf{X}}_{\widetilde{p}}^T \widetilde{\mathbf{X}}_{\widetilde{p}}\right)^{-1} \widetilde{\mathbf{X}}_{\widetilde{p}}^T \mathbf{Y}_q. \tag{4}$$

The estimated $\hat{\mathbf{Y}}_q$ in (4) are computed in four steps: *(i)* orthonormal bases $\left\{\Psi_j\right\}_{j=1}^{p}$ and $\left\{\Phi_k\right\}_{k=1}^{q}$ are defined as the (empirical) FPC of $\mathcal{X}$ and $\mathcal{Y}$, respectively (in what follows, $\left\{\Psi_j\right\}_{j=1}^{p}$ and $\left\{\Phi_k\right\}_{k=1}^{q}$ are the eigenfunctions of the empirical covariance operators $C_n^{\mathcal{X}}$ and $C_n^{\mathcal{Y}}$, respectively); *(ii)* initial values (p,q) are fixed (for a particular sample) with regard to a certain proportion of Explained Variance EV_p and EV_q (say $\mathrm{EV}_p = \mathrm{EV}_q \geq 0.99$), where $\mathrm{EV}_p = \sum_{j=1}^{p} \lambda_j^{\Psi}$ and $\mathrm{EV}_q = \sum_{k=1}^{q} \lambda_k^{\Phi}$, being $\left\{\lambda_j^{\Psi}\right\}_{j=1}^{p}$ and $\left\{\lambda_k^{\Phi}\right\}_{k=1}^{q}$ the associated eigenvalues; *(iii)* a variable selection is implemented, based on a LASSO (L1) regularization, by considering the no null rows of $\hat{\mathbf{B}}_{p,q}^{(\lambda)} =$

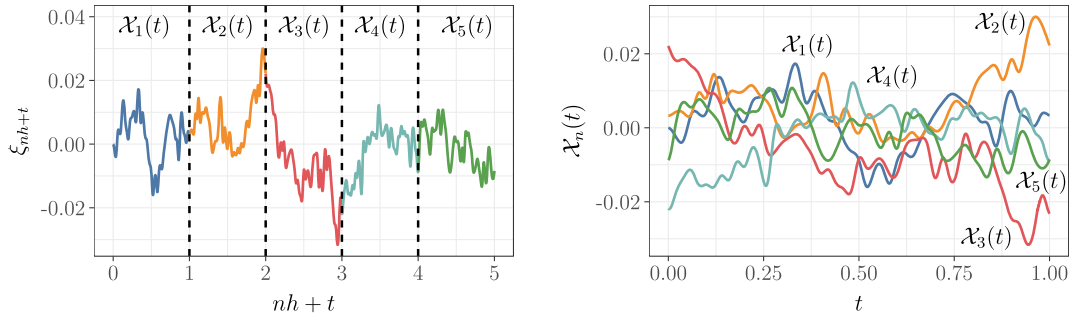

(a) *Continuous path of an stochastic process* $\{\xi_t\}_{t\in\mathbb{R}^+}$*, splitted into* $[0,h]$ *(*$h=1$*), such that* $\mathcal{X}_i(t)=\xi_{ih+t}$.

(b) *The same stochastic process characterized as a set of ARH(1) trajectories* $\{\mathcal{X}_n(t)\colon t\in[0,1]\}_{i=1,\dots,n}$*, with* $n=5$.

Fig. 1. Stochastic process $\{\xi_t\}_{t\in\mathbb{R}^+}$ characterized and splitted as an ARH(1) process.

$\arg\min_{\mathbf{B}_{p,q}}\left\{\frac{1}{2n}\sum_{i=1}^{n}\left\|\left(\mathbf{Y}_q\right)_i-\left(\mathbf{X}_p\mathbf{B}_{p,q}\right)_i\right\|^2+\lambda\sum_{j=1}^{p}\left\|\left(\mathbf{B}_{p,q}\right)_j\right\|_2\right\}$, being $\left(\mathbf{Y}_q\right)_i$ the i-th row of $\mathbf{Y}_q$; *(iv)* a FPCR estimation is performed just using the set of $\widetilde{p}\le p$ predictors selected, whose coefficients are denoted as $\widetilde{\mathbf{X}}_{\widetilde{p}}$, and therefore, having a hat matrix $\mathbf{H}_C^{(\lambda)}$ at our disposal, which will be crucial within the bootstrap algorithm.

Hence, the FPCR-L1-selected (FPCR-L1S) estimator in (4) allows us to seize the advantages of both estimation paradigms. This estimator critically depends on the penalty parameter λ. Whilst $\hat{\lambda}_{CV}$ (leave-one-out cross-validation) is an optimal choice for estimating β, the so-called one standard error rule (see Friedman et al., 2010) is adopted, denoted in the GoF folklore as $\hat{\lambda}_{1SE}$ (a variance reduction is achieved to obtain a more biased estimator for test calibration). Both approaches were implemented in the R package goffda (García-Portugués and Álvarez-Liébana, 2019). Estimator in (4) could be extended to non orthonormal bases, just replacing $\mathbf{X}_p$ by $\check{\mathbf{X}}_p=\mathbf{X}_p\mathbf{\Psi}$ in (3), where $\mathbf{\Psi}=\left\{\langle\Psi_j,\Psi_j\rangle_{\mathbb{H}_1}\right\}_{i,j=1,\dots,p}$.

Note that the current proposal is based on the assumption that the curves are represented on an equally spaced grid, as is commonly assumed in the context of diffusion processes. More detailed aspects about it can be found in Section 6.

2.2. Functional time series: autoregressive Hilbertian processes

Since the underlying idea of the methodology proposed in Section 3 revolves around characterizing ARH processes as a specific case of FLMFR, we will first present some preliminary elements of these models from a time-domain perspective. Given a probability space $(\Omega,\mathcal{A},\mathbb{P})$, let $\{\xi_t\}_{t\in\mathbb{R}}$ be now a continuous-time zero-mean stochastic process. In keeping with Bosq (2000), the paths are splitted as $\mathcal{X}_n(t)=\xi_{nh+t}$, with $t\in[0,h]$, and $\mathcal{X}_n\in\mathbb{H}=L^2([0,h])$, for each $n\in\mathbb{Z}$, constituting an infinite-dimensional discrete-time process. This representation (see Fig. 1) is especially fruitful if $\{\xi_t\}_{t\in\mathbb{R}}$ displays a seasonal component either it will be forecasted over $[0,h]$. Henceforth, $\mathcal{X}=\{\mathcal{X}_n\}_{n\in\mathbb{Z}}$ is a zero-mean autoregressive Hilbertian process of order one, valued in $\mathbb{H}=L^2([0,h])$, denoted as ARH(1), if the following state equation is satisfied

$$\mathcal{X}_n(t)=\rho\left(\mathcal{X}_{n-1}\right)(t)+\mathcal{E}_n(t),\quad n\in\mathbb{Z},\quad \mathcal{X}_n,\ \mathcal{E}_n\in\mathbb{H}=L^2([0,h]),\quad t\in[0,h], \tag{5}$$

where $\rho\equiv\rho_\beta$ denotes the linear autocorrelation operator, with $\|\rho\|_{\mathcal{L}(\mathbb{H})}=\sup_{\|\mathcal{X}\|_{\mathbb{H}}\le1}\|\rho(\mathcal{X})\|_{\mathbb{H}}$, and $\varepsilon=\{\mathcal{E}_n\}_{n\in\mathbb{Z}}$ is assumed to be a strong-white noise, that is, from Bosq (2000), ε is then a zero mean $\mathbb{H}$-valued stationary process with independent and identically distributed (iid) components and $\sigma^2=\mathrm{E}\left[\|\varepsilon_n\|_{\mathbb{H}}^2\right]<\infty$, uncorrelated with the random initial condition. The subsequent assumptions will be considered:

Assumption 1. $\|\rho^k\|_{\mathcal{L}(\mathbb{H})}<1$, for any $k\ge k_0$, and for some $k_0\ge1$, where ρ^k denotes the composition operator $\rho\overbrace{\circ\cdots\circ}^{k}\rho$, leading to $\sum_{n=0}^{\infty}\|\rho^n\|_{\mathcal{L}(\mathbb{H})}<\infty$.

Assumption 2. The autocorrelation operator is given by $\rho_\beta(\mathcal{X})(t)=\int_0^h\beta(s,t)\mathcal{X}(s)\mathrm{d}s$, with $\beta=\sum_{j=1}^{\infty}\sum_{k=1}^{\infty}\beta_{jk}\Psi_j\otimes\Psi_k$, such that $\iint\beta^2(s,t)\mathrm{d}s\mathrm{d}t<\infty$ (Hilbert–Schmidt integral operator) and $\beta_{jk}=\langle\beta,\Psi_j\otimes\Psi_k\rangle_{\mathbb{H}}$, for each $j,k=1,\dots,\infty$.

Remark that the autocovariance operator $C := \mathrm{E}[\mathcal{X}_n \otimes \mathcal{X}_n]$ is a self-adjoint, trace and positive operator, for each $n \in \mathbb{Z}$. As a result, it admits a diagonal FPC-based decomposition $C = \sum_{j=1}^{\infty} C_j \Psi_j \otimes \Psi_j$, being $\{\Psi_j\}_{j=1}^{\infty}$ the theoretical eigenfunctions of C, associated with eigenvalues $C_1 \geq \ldots \geq C_j \geq \ldots > 0$. From Bosq (2000, Theorem 3.1), Assumption 1 is required for ensuring an unique stationary solution. Since $C^{-1} = \sum_{j=1}^{\infty} \frac{1}{C_j} \Psi_j \otimes \Psi_j$, under the trace property, C cannot be inverted, and thus, $\rho := DC^{-1}$ should be estimated. Note that Assumption 2 does not imply that DC^{-1} could be diagonally decomposed, since the symmetry of the cross-covariance operator $D := \mathrm{E}\left[\mathcal{X}_n \otimes \mathcal{X}_{n+1}\right]$ is not imposed.

Remark 1. As a sideways contribution, a strongly consistent estimator of ρ, under weaker conditions that those ones in Bosq (2000), can be found in the Supplementary Material, improving the decay rate of convergence of the associated predictor. The estimation under the compactness of D was achieved in Álvarez-Liébana et al. (2017).

3. A GoF test for functional autoregressive processes

A new GoF test for ARH processes, against unspecified alternative, is now proposed. Firstly, it is extended the ARH(1) process in Section 2.2 to ARH(z) models, even with $z > 1$. Secondly, these ARH(z) processes are characterized as a particular case of FLMFR, under the setting established in Section 2.1. Lastly, it is detailed the GoF test proposal for ARH(z) processes, from a FLMFR perspective, and implemented a simulation study.

3.1. ARH(z) processes: state equation

The Markovianess of the ARH(1) model in (5) allows us to easily generalized it by including more lagged functional regressors, i.e., $\mathcal{X}_n$ is inferred from $(\mathcal{X}_{n-1}, \ldots, \mathcal{X}_{n-z})$. Formally, $\mathcal{X} = \{\mathcal{X}_n\}_{n\in\mathbb{Z}}$ is a zero-mean autoregressive Hilbertian process of order $z \geq 1$, valued in $\mathbb{H} = L^2([0,h])$ and denoted as ARH(z), if the following state equation is satisfied:

$$\mathcal{X}_n(t) = \sum_{r=1}^{z} \rho_r\left(\mathcal{X}_{n-r}\right)(t) + \mathcal{E}_n(t), \quad z \geq 1, \quad \mathcal{X}_n, \mathcal{E}_n \in \mathbb{H}, \quad t \in [0,h], \quad n \in \mathbb{Z}, \tag{6}$$

where $\{\rho_r\}_{r=1}^{z}$ are bounded linear operators in $\mathcal{L}(\mathbb{H})$, and $\varepsilon = \{\mathcal{E}_n\}_{n\in\mathbb{Z}}$ is a $\mathbb{H}$-valued strong white noise, such that $\mathbb{P}\left(\rho_z\left(\mathcal{X}_n\right) \neq 0\right) > 0$ is implicitly assumed, for each $n \in \mathbb{Z}$.

ARH(1) estimation results can be effortlessly extended to this context since ARH(z) process in (6) can be reinterpreted a particular multivariate ARH(1) process, valued in $\mathbb{H}^z := \prod_{r=1}^{z} \mathbb{H}$, constituting likewise a separable Hilbert space (see Lemma 1 in the Supplementary Material). In this way, the following proposition allows us to characterize the ARH(z) in (6) as a $\mathbb{H}^z$-valued stationary ARH(1) process. See proofs in the Supplementary Material.

Proposition 1. *Let $\mathcal{X} := \{\mathcal{X}_n\}_{n\in\mathbb{Z}}$ be a zero-mean ARH(z) process valued in $\mathbb{H} = L^2([0,h])$, with $z \geq 1$. The ARH(z) model in (6) can be reinterpreted as*

$$\underline{\mathcal{X}}_n = \begin{pmatrix} \mathcal{X}_n \\ \vdots \\ \mathcal{X}_{n-z+1} \end{pmatrix} \in \mathbb{H}^z, \quad \underline{\rho} = \begin{pmatrix} \rho_1 & \cdots & \rho_{z-1} & \rho_z \\ Id_{\mathbb{H}} & \cdots & 0_{\mathbb{H}} & 0_{\mathbb{H}} \\ \vdots & \ddots & \vdots & \vdots \\ 0_{\mathbb{H}} & \cdots & Id_{\mathbb{H}} & 0_{\mathbb{H}} \end{pmatrix}, \quad \underline{\mathcal{E}}_n = \left(\mathcal{E}_n, \mathbf{0}, \ldots, \mathbf{0}\right)^T \in \mathbb{H}^z, \tag{7}$$

where $\mathbb{H}^z$ is the Cartesian product of z copies of $\mathbb{H}$. Thus, $\underline{\mathcal{X}}_n = \underline{\rho}\left(\underline{\mathcal{X}}_{n-1}\right) + \underline{\mathcal{E}}_n$, constitutes a $\mathbb{H}^z$-valued ARH(1) process, for each $n \in \mathbb{Z}$, with $\underline{\mathcal{E}}_n$ a $\mathbb{H}^z$-valued strong white noise. Furthermore, the joint operator $\underline{\rho}$ is also a bounded linear operator in $\mathbb{H}^z$. In (7), $Id_{\mathbb{H}}$ and $0_{\mathbb{H}}$ denote the identity and null operators, respectively, and $\mathbf{0}$ the null element on $\mathbb{H}$.

Concerning Assumption 1 (commonly assumed, see e.g. Bosq 2000), a sufficient condition for the existence of an unique stationary solution of (6) is provided in Proposition 2 below. It is therein proved that the stationarity condition in the ARH(z) context can be verified just requesting that their multivariate formulation (as a matrix of operators defined in (7)) as in the ARH(1) case.

Proposition 2. *Let $\mathcal{X} = \{\mathcal{X}_n\}_{n\in\mathbb{Z}}$ be a zero-mean ARH(z) process, with $z \geq 1$, as explicitly defined in (6)–(7). If $\left\|\underline{\rho}^k\right\|_{\mathcal{L}(\mathbb{H}^z)} < 1$, for any $k \geq k_0$, and for some $k_0 \geq 1$, then the state equation established in (6) has a unique stationary solution given by $\mathcal{X}_n = \sum_{j=0}^{\infty} \Pi_1\left(\underline{\rho}^j\left(\underline{\mathcal{E}}_{n-j}\right)\right)$, for each $n \in \mathbb{Z}$, where $\Pi_r : \left(\mathcal{X}_{(1)}, \ldots, \mathcal{X}_{(z)}\right) \mapsto \mathcal{X}_{(r)}$, with $r = 1, \ldots, z$.*

Remark 2. As proved in Lemma 2 in the Supplementary Material, Assumption 1 on $\underline{\rho}$ also implies that Assumption 1 is held for each ρ_r, with $r = 1, \ldots, z$ (i.e., stationarity condition in Proposition 2 leads to $\sum_{n=0}^{\infty} \left\|\rho_r^n\right\|_{\mathcal{L}(\mathbb{H})} < \infty$). Remark also that, from the definition of norm $\|\cdot\|_{\mathbb{H}^z}$, Assumption 2 on $\underline{\rho}$ is verified as long as Assumption 2 is satisfied for each ρ_r, for any $r = 1, \ldots, z$. Note that now $\underline{C} := \mathrm{E}\left[\underline{\mathcal{X}}_n \otimes_{\mathbb{H}^z} \underline{\mathcal{X}}_n\right]$ is the autocovariance operator, where $\otimes_{\mathbb{H}^z}$ denotes the tensor product on $\mathbb{H}^z$, given by

$$\underline{C}(\underline{\mathcal{X}}) = \sum_{j=1}^{\infty} \underline{C}_j \underline{\Psi}_j \left\langle \underline{\Psi}_j, \underline{\mathcal{X}} \right\rangle_{\mathbb{H}^z}, \quad \left\langle \underline{C}(\underline{\mathcal{X}}), \underline{\mathcal{Y}} \right\rangle_{\mathbb{H}^z} = \sum_{j=1}^{\infty} \underline{C}_j \left\langle \underline{\Psi}_j, \underline{\mathcal{X}} \right\rangle_{\mathbb{H}^z} \left\langle \underline{\Psi}_j, \underline{\mathcal{Y}} \right\rangle_{\mathbb{H}^z}, \quad \underline{\mathcal{X}}, \underline{\mathcal{Y}} \in \mathbb{H}^z,$$

where $\left\{\underline{\Psi}_j\right\}_{j=1}^{\infty}$ and $\left\{\underline{C}_j\right\}_{j=1}^{\infty}$ denote their $\mathbb{H}^z$-valued FPC and their eigenvalues, respectively. The joint operator $\underline{C}$ can be re-interpreted as $\underline{C} = \left(C_{r,s}\right)_{r=1,\dots,z}^{s=1,\dots,z}$, where $C_{r,s} = \mathrm{E}\left[\mathcal{X}_{n,(r)} \otimes \mathcal{X}_{n,(s)}\right]$, being $\mathcal{X}_{n,(r)}$ the r-th element of $\underline{\mathcal{X}}_n$, for each $n \in \mathbb{Z}$ and $r = 1, \dots, z$.

3.2. ARH(z) processes characterized as FLMFR

Although a strongly consistent estimator of ρ in the ARH setting is provided in the Supplementary Material, its formulation can be quite complex. This complexity arises from the intricacies of the estimator itself. Furthermore, the lack of an explicit hat matrix significantly increases the computational cost of the procedure. For these reasons, an alternative characterization of the ARH(z) model in (6), based on properties detailed in Section 3.1, is now suggested, re-expressed it as a FLMFR. As commented, from Remark 2, under Assumption 2 on each $\left\{\rho_r\right\}_{r=1}^{z}$,

$$\rho_r\left(\mathcal{X}\right)(t) = \int_0^h \beta_r(s,t)\mathcal{X}(s)\mathrm{d}s, \quad \beta_r = \sum_{j=1}^{\infty}\sum_{k=1}^{\infty} \beta_{jk}^{(r)} \Psi_j \otimes \Psi_k, \quad \int_0^h \int_0^h \beta_r^2(s,t)\mathrm{d}s\mathrm{d}t < \infty. \tag{8}$$

Given a zero-mean ARH(z) process in (6), $\widetilde{\mathcal{X}}_n(s) = \sum_{r=1}^{z} \mathcal{X}_{n-r}\left(sz-(r-1)\right)\mathbb{1}_r(s)$, for each $s \in [0,h]$, where $\mathbb{1}_r(\cdot) := \mathbb{1}_{\left[\frac{(r-1)h}{z}, \frac{rh}{z}\right]}(\cdot)$ denotes the indicator function in $\left[\frac{(r-1)h}{z}, \frac{rh}{z}\right]$, for each $r = 1, \dots, z$. In the same way, a change of variable $x := (s+r-1)/z$ yields

$$\rho_r\left(\mathcal{X}_{n-r}\right)(t) = \int_0^h \beta_r(s,t)\mathcal{X}_{n-r}(s)\mathrm{d}s = z \int_{\frac{(r-1)h}{z}}^{\frac{rh}{z}} \beta_r(xz-(r-1),t)\mathcal{X}_{n-r}(xz-(r-1))\mathrm{d}x,$$

for each $r = 1, \dots, z$ and $t \in [0,h]$, and then,

$$\begin{aligned}\sum_{r=1}^{z} \rho_r\left(\mathcal{X}_{n-r}\right)(t) &= \sum_{r=1}^{z} z \int_{\frac{(r-1)h}{z}}^{\frac{rh}{z}} \beta_r(xz-(r-1),t)\mathcal{X}_{n-r}(xz-(r-1))\mathrm{d}x \\ &= \int_0^h \left[z\sum_{r=1}^{z} \beta_r(sz-(r-1),t)\mathbb{1}_r(s)\right]\left[\sum_{r=1}^{z} \mathcal{X}_{n-r}(sz-(r-1))\mathbb{1}_r(s)\right]\mathrm{d}s,\end{aligned}$$

such that

$$\sum_{r=1}^{z} \rho_r\left(\mathcal{X}_{n-r}\right)(t) = \int_0^h \widetilde{\beta}(s,t)\widetilde{\mathcal{X}}_n(s)\mathrm{d}s, \quad \widetilde{\beta}(s,t) = z\sum_{r=1}^{z} \beta_r(sz-(r-1),t)\mathbb{1}_r(s), \tag{9}$$

and $\widetilde{\mathcal{X}}_n(s) = \sum_{r=1}^{z} \mathcal{X}_{n-r}(sz-(r-1))\mathbb{1}_r(s)$, such that under Assumption 2, the inequality $\int_0^h \int_0^h \widetilde{\beta}^2(s,t)\mathrm{d}s\mathrm{d}t \le z\sum_{r=1}^{z} \int_0^h \int_0^h \beta_r^2(s,t)\mathrm{d}s\mathrm{d}t < \infty$, as long as $z < \infty$, is held. Hence, the previous inequality lies on the FLMFR setting detailed in Section 2.1, under Assumptions 1–2, which ensure us the stationarity. Given a sample of a zero-mean ARH(z) process $\left\{\mathcal{X}_i\right\}_{i=0}^{n-1+z}$ valued in $\mathbb{H} = L^2([0,h])$, then for each $i = 1, \dots, n$,

$$\widetilde{\mathcal{Y}}_i = \widetilde{\rho}\left(\widetilde{\mathcal{X}}_i\right) + \widetilde{\mathcal{E}}_i, \quad \mathrm{E}\left[\widetilde{\mathcal{E}}_i \,\middle|\, \widetilde{\mathcal{X}}_i\right] = 0, \quad \widetilde{\rho}(x) = \mathrm{E}\left[\widetilde{\mathcal{Y}} \,\middle|\, \widetilde{\mathcal{X}} = x\right] : \mathbb{H} \mapsto \mathbb{H}, \tag{10}$$

where $\widetilde{\mathcal{X}}_i = \sum_{r=1}^{z} \mathcal{X}_{z-r+(i-1)}(sz-(r-1))\mathbb{1}_r(s)$, and $\widetilde{\mathcal{Y}}_i := \mathcal{X}_{(i-1)+z}$ and $\widetilde{\mathcal{E}}_i := \mathcal{E}_{(i-1)+z}$, for each $i = 1, \dots, n$, all of them centered. From (8)–(10),

$$\widetilde{\rho}(\mathcal{X})(\cdot) = \int_0^h \widetilde{\beta}(s,\cdot)\mathcal{X}(s)\mathrm{d}s \quad \text{Hilbert-Schmidt operator}, \quad \widetilde{\beta} = \sum_{j=1}^{\infty}\sum_{k=1}^{\infty} \widetilde{\beta}_{jk}\Psi_j \otimes \Psi_k, \tag{11}$$

where $\widetilde{\boldsymbol{\rho}}_{\widetilde{p},q} = \left(\widetilde{\beta}_{jk}\right)_{j=1,\dots,\widetilde{p}}^{k=1,\dots,q}$ is the $\widetilde{p}\times q$ matrix of the coefficients of $\widetilde{\beta}_{jk} = \langle \widetilde{\beta}, \Psi_j \otimes \Psi_k \rangle_{\mathbb{H}^z}$, being $\widetilde{\beta}$ defined in (9). Now, $\left\{\Psi_j \otimes \Psi_k\right\}_{j,k=1}^{\widetilde{p},q}$ is constituted by the truncated versions of the same functional basis $\left\{\Psi_j\right\}_{j=1}^{\infty}$, although different cut-off levels $\left(\widetilde{p}, q\right)$ might be required. Note that, even though $\mathcal{X}_i$ and $\mathcal{E}_i$ are correlated, $\mathrm{E}\left[\widetilde{\mathcal{E}}_i \,\middle|\, \widetilde{\mathcal{X}}_i\right] = 0$, for each $i = 1, \dots, n$, since $\left(\mathcal{X}_{n-1}, \dots, \mathcal{X}_{n-z}\right)$ and $\mathcal{E}_n$ are uncorrelated, for each $n \in \mathbb{Z}$. Since the previous z-lagged values are used, $\left\{\mathcal{X}_i\right\}_{i=0}^{n-1+z}$ are required for computing $\left\{\widetilde{\mathcal{X}}_i\right\}_{i=1}^{n}$.

Remark 3. Concerning to the case where $\widetilde{\rho}$ is furthermore compact, Assumption 2 could be modified, since $\widetilde{\rho}$ would admit a diagonal spectral decomposition in terms of an infinite sequence of real–valued AR(1) state equations, after projection the fully functional trajectories into the set of eigenfunctions of autocovariance operator (see, e.g., Salmerón and Ruiz-Medina, 2009 and Ruiz-Medina and Salmerón, 2010). In that case, it could be extended in a direct way the asymptotic results by Koul and Stute (1999) for the real–valued case, such that considering ARH processes in terms of generalized processes (see Gelfand and Vilenkin, 1964), the weak–convergence of the projected empirical processes to a two–parameter generalized continuous Gaussian process may be achieved. This process would admit in distribution sense a representation, in terms of two–parameter generalized Brownian motion.

3.3. A GoF test for ARH(z) models

As exposed, the guiding thread of this paper is to verify whether the relation between frv's $\left\{\widetilde{\mathcal{Y}}_i=\mathcal{X}_{i-1+z}\right\}_{i=1}^{n}$ and their z-lagged values $\left\{\left(\mathcal{X}_{z-1+(i-1)},\mathcal{X}_{z-2+(i-1)},\ldots,\mathcal{X}_{(i-1)}\right)\right\}_{i=1}^{n}$ can be linearly related. For this purpose, a GoF test for the ARH(z) model in (6) is now formulated, based on its characterization as a FLMFR. Particularly, for a given $z\geq 1$, it is tested the composite null hypothesis $\mathcal{H}_0$ (against an unspecified alternative)

$$\mathcal{H}_0:\ \mathcal{X}_n \text{ and } \left(\mathcal{X}_{n-1},\ldots,\mathcal{X}_{n-z}\right) \text{ are linearly related},\quad n\in\mathbb{Z}. \tag{12}$$

Note the reader that, from Proposition 1, the null hypothesis $\mathcal{H}_0$ in (12) is equivalent to

$$\mathcal{H}_0:\ \underline{\mathcal{X}}_n=\underline{\rho}\left(\underline{\mathcal{X}}_{n-1}\right)+\underline{\mathcal{E}}_n,\quad \underline{\rho}\left(\underline{\mathcal{X}}\right)(t):=\underline{\rho}_{\underline{\beta}}\left(\underline{\mathcal{X}}\right)(t)=\left\langle\underline{\beta}(\cdot,t),\underline{\mathcal{X}}(\cdot)\right\rangle_{\mathbb{H}^z},\quad \underline{\mathcal{X}}\in\mathbb{H}^z, \tag{13}$$

with $n\in\mathbb{Z}$, for some unknown squared-integrable $\underline{\beta}\in\mathbb{H}^z\otimes_{\mathbb{H}^z}\mathbb{H}^z$, where $\mathbb{H}^z$ is a separable Hilbert space, as proved in Lemma 1 in the Supplementary Material. Furthermore, from Section 3.2, $\mathcal{H}_0$ in (12)–(13) is also equivalent to

$$\mathcal{H}_0:\ \widetilde{\rho}\in\mathcal{L}=\left\{\langle\langle\cdot,\widetilde{\beta}\rangle\rangle:\ \widetilde{\beta}\in\mathbb{H}\otimes\mathbb{H}\right\},\quad \widetilde{\mathcal{Y}}=\widetilde{\rho}\left(\widetilde{\mathcal{X}}\right)+\widetilde{\mathcal{E}},\quad \widetilde{\rho}_{\widetilde{\beta}}\left(\widetilde{\mathcal{X}}\right)(t)=\int_0^h\widetilde{\beta}(s,t)\widetilde{\mathcal{X}}(s)\mathrm{d}s, \tag{14}$$

where $\widetilde{\mathcal{X}}_i=\sum_{r=1}^{z}\mathcal{X}_{z-r+(i-1)}(sz-(r-1))\mathbb{1}_r(s)$, and $\widetilde{\mathcal{Y}}_i:=\mathcal{X}_{i-1+z}$ and $\widetilde{\mathcal{E}}_i:=\mathcal{E}_{i-1+z}$ centered frv's, for each $i=1,\ldots,n$, being $\widetilde{\rho}$ a Hilbert-Schmidt integral operator. In what follows, the characterization of null hypothesis $\mathcal{H}_0$ in (14) from a FLMFR perspective, based on developments in (8)–(11), is considered.

From García-Portugués et al. (2021, Lemmas 1-2), the null hypothesis in (14) can be also characterized in terms of the projections of the functional paths as follows

$$\mathcal{H}_0:\ \mathrm{E}\left[\langle\widetilde{\mathcal{Y}}-\langle\langle\widetilde{\mathcal{X}},\widetilde{\beta}\rangle\rangle,\rho_{\widetilde{\mathcal{Y}}}\rangle_{\mathbb{H}}\mathbb{1}_{\left\{\langle\widetilde{\mathcal{X}},\rho_{\widetilde{\mathcal{X}}}\rangle_{\mathbb{H}}\leq u\right\}}\right]=0,\quad \text{for almost every } u\in\mathbb{R},$$

and for each direction $\rho_{\widetilde{\mathcal{X}}},\rho_{\widetilde{\mathcal{Y}}}\in\mathbb{S}_{\mathbb{H}}$, where $\mathbb{S}_{\mathbb{H}}=\left\{\mathcal{X}\in\mathbb{H}:\ \|\mathcal{X}\|_{\mathbb{H}}=1\right\}$ is the functional analogue of the Euclidean sphere. Extending the ideas of Escanciano (2006), deviations from $\mathcal{H}_0$ can be detected by computing a residual marked empirical process

$$R_n\left(u,\rho_{\widetilde{\mathcal{X}}},\rho_{\widetilde{\mathcal{Y}}}\right)=\frac{1}{\sqrt{n}}\sum_{i=1}^{n}\langle\widetilde{\mathcal{E}}_i,\rho_{\widetilde{\mathcal{Y}}}\rangle_{\mathbb{H}}\mathbb{1}_{\left\{\langle\widetilde{\mathcal{X}},\rho_{\widetilde{\mathcal{X}}}\rangle_{\mathbb{H}}\leq u\right\}},\quad u\in\mathbb{R},\quad \rho_{\widetilde{\mathcal{X}}},\rho_{\widetilde{\mathcal{Y}}}\in\mathbb{S}_{\mathbb{H}},$$

where marks are given by the projected errors $\left\{\langle\widetilde{\mathcal{E}}_i,\rho_{\widetilde{\mathcal{Y}}}\rangle_{\mathbb{H}}=\langle\widetilde{\mathcal{Y}}_i-\langle\langle\widetilde{\mathcal{X}}_i,\hat{\beta}\rangle\rangle,\rho_{\widetilde{\mathcal{Y}}}\rangle_{\mathbb{H}}\right\}_{i=1}^{n}$ and jumps are determined by the projected regressors $\left\{\langle\widetilde{\mathcal{X}}_i,\rho_{\widetilde{\mathcal{X}}}\rangle_{\mathbb{H}}\right\}_{i=1}^{n}$, where $\hat{\beta}$ denotes some estimator of $\widetilde{\beta}$ (see equations (8)–(11)). To measure how close the empirical process is to zero, a projected Cramér–von Mises (PCvM) statistic, on the norm on $\mathbb{S}_{\mathbb{H}}\times\mathbb{S}_{\mathbb{H}}\times\mathbb{R}$, will be adopted as

$$\mathrm{PCvM}_n=\int_{\mathbb{S}_{\mathbb{H}}\times\mathbb{S}_{\mathbb{H}}\times\mathbb{R}}\left[R_n\left(u,\rho_{\widetilde{\mathcal{X}}},\rho_{\widetilde{\mathcal{Y}}}\right)\right]^2F_{n,\rho_{\widetilde{\mathcal{X}}}}(\mathrm{d}u)\omega_{\widetilde{\mathcal{X}}}(\mathrm{d}\rho_{\widetilde{\mathcal{X}}})\omega_{\widetilde{\mathcal{Y}}}(\mathrm{d}\rho_{\widetilde{\mathcal{Y}}}),$$

where $F_{n,\rho_{\widetilde{\mathcal{X}}}}$ is the empirical cumulative distribution function (ecdf) of projected regressors, and $\omega_{\widetilde{\mathcal{X}}}$ and $\omega_{\widetilde{\mathcal{Y}}}$ are suitable measures on $\mathbb{S}_{\mathbb{H}}$, respectively. The infinite dimension of functional spheres makes this functional hard to handle. For that reason, the projected Cramér-von Mises statistic will be expressed in terms of finite-dimensional directions $\rho_{\widetilde{\mathcal{X}}}^{(\widetilde{p})}$ and $\rho_{\widetilde{\mathcal{Y}}}^{(q)}$, as well as $\widetilde{\mathcal{E}}_i^{(q)}$ and $\widetilde{\mathcal{X}}^{(\widetilde{p})}$, just adopting a $(\widetilde{p},\mathrm{q})$-truncated expansions. After some simple algebra developments, an easily computable statistic was obtained as

$$\mathrm{PCvM}_{n,\widetilde{p},q}=\frac{1}{n^2}\frac{2\pi^{\widetilde{p}/2+q/2-1}}{q\Gamma(\widetilde{p}/2)\Gamma(q/2)}\mathrm{Tr}\left[\widetilde{\mathbf{E}}_q^T\mathbf{A}_{\bullet}\widetilde{\mathbf{E}}_q\right],\quad \left(\widetilde{\mathbf{E}}_q\right)_{i=1,\ldots,n}^{k=1,\ldots,q}=\hat{e}_{i,k}=\langle\widetilde{\mathcal{E}}_i,\Psi_k\rangle_{\mathbb{H}}, \tag{15}$$

being $\mathrm{Tr}[\cdot]$ the trace operator, $\Gamma(\cdot)$ the Gamma function and $\widetilde{\mathbf{E}}_q$ the error coefficients, that is, the projected estimators of $\widetilde{\mathcal{E}}_i:=\mathcal{E}_{i-1+z}$, for each $i=1,\ldots,n$. The matrix $\mathbf{A}_{\bullet}=\left(\mathbf{A}_{\bullet}\right)_{ij}=\left(\sum_{r=1}^{n}A_{ijr}\right)_{ij}$ is obtained as surface areas of particular spherical regions, which explicit expression can be given as (see García-Portugués et al., 2014 and García-Portugués et al., 2021)

$$A_{ijr} = A^{\measuredangle}_{ijr}\frac{\pi^{\widetilde{p}/2-1}}{\rho(\widetilde{p}/2)}, \quad A^{\measuredangle}_{ijr} := \begin{cases} 2\pi, & \boldsymbol{x}_{i,\widetilde{p}} = \boldsymbol{x}_{j,\widetilde{p}} = \boldsymbol{x}_{r,\widetilde{p}} \\ \pi, & \boldsymbol{x}_{i,\widetilde{p}} \neq \boldsymbol{x}_{j,\widetilde{p}}, \text{ and } \boldsymbol{x}_{i,\widetilde{p}} = \boldsymbol{x}_{r,\widetilde{p}} \text{ or } \boldsymbol{x}_{j,p} = \boldsymbol{x}_{i,\widetilde{p}} \\ \pi - \cos^{-1}\left(\frac{(\boldsymbol{x}_{i,\widetilde{p}}-\boldsymbol{x}_{r,\widetilde{p}})^T(\boldsymbol{x}_{j,\widetilde{p}}-\boldsymbol{x}_{r,\widetilde{p}})}{\|\boldsymbol{x}_{i,\widetilde{p}}-\boldsymbol{x}_{r,\widetilde{p}}\|\|\boldsymbol{x}_{j,\widetilde{p}}-\boldsymbol{x}_{r,\widetilde{p}}\|}\right), \end{cases} \tag{16}$$

where $\boldsymbol{x}_{i,\widetilde{p}} = \left(\langle \mathcal{X}_i, \Psi_1\rangle, \ldots, \langle \mathcal{X}_i, \Psi_{\widetilde{p}}\rangle\right)^T$. Geometrical arguments $\left(A_{ijr}\right)_{i,j,r=1,\ldots,n}$ can be directly computed from the R package goffda (García-Portugués and Álvarez-Liébana, 2019), and they depend exclusively on the covariates, and then, they only needs to be computed once in the testing procedure. The GoF test for ARH(z) models proposed is then detailed within the next algorithm.

Algorithm 1 *(GoF test in practice).* Let $\{\mathcal{X}_i\}_{i=0}^{n-1+z}$ be a sample of a centered ARH(z) model, under Assumptions 1–2 and the setting above detailed. It proceeds as follows:

1. Construct frv's $\widetilde{\mathcal{X}}_i(s) := \sum_{r=1}^{z} \mathcal{X}_{z-r+(i-1)}(sz-(r-1))\mathbb{1}_r(s)$, $\widetilde{\mathcal{Y}}_i(t) := \mathcal{X}_{(i-1)+z}(t)$ and $\widetilde{\mathcal{E}}_i(t) := \mathcal{E}_{(i-1)+z}(t)$, all of them centered, with $\widetilde{\mathcal{Y}}_i = \widetilde{\rho}\left(\widetilde{\mathcal{X}}_i\right) + \widetilde{\mathcal{E}}_i$, for any $i = 1, \ldots, n$, and $s, t \in [0, h]$, constituting a particular case of FLMFR.
2. Compute the FPC of $\left\{\widetilde{\mathcal{X}}_i\right\}_{i=1}^{n}$ and $\left\{\widetilde{\mathcal{Y}}_i\right\}_{i=1}^{n}$, and choose initial cut-off levels (p, q) as the minimum number of FPC required for capturing a proportion of EV (say $\mathrm{EV}_p = \mathrm{EV}_q = 0.99$). After that, the p- and q-truncated FPC scores $\widetilde{\mathbf{X}}_p$ and $\widetilde{\mathbf{Y}}_q$ of $\left\{\widetilde{\mathcal{X}}_i\right\}_{i=1}^{n}$ and $\left\{\widetilde{\mathcal{Y}}_i\right\}_{i=1}^{n}$, are obtained, respectively.
3. Compute the FPCR-L1S estimator $\widehat{\widetilde{\mathbf{B}}}^{(\lambda),C}_{\widetilde{p},q}$ of $\widetilde{\mathbf{B}}_{\widetilde{p},q}$, where $\widetilde{\mathbf{B}}_{\widetilde{p},q} = \left(\widetilde{\beta}_{jk}\right)_{j=1,\ldots,\widetilde{p}}^{j=1,\ldots,q}$ is the $\widetilde{p}\times q$ matrix of the coefficients of $\widetilde{\beta}_{jk} = \langle \widetilde{\beta}, \Psi_j \otimes \Psi_k\rangle_{\mathbb{H}^z}$, and the associated coefficients of residuals $\widetilde{\mathbf{e}}_{i,q} = \widetilde{\mathbf{Y}}_{i,q} - \widetilde{\mathbf{X}}_{i,\widetilde{p}}\widehat{\widetilde{\mathbf{B}}}^{(\lambda),C}_{\widetilde{p},q}$, for each $i = 1, \ldots, n$. Note that $\widetilde{p}$ out of p FPC coefficients are automatically selected. The statistic $\mathrm{PCvM}_{n,\widetilde{p},q}$ in (15) is computed.
4. Implement a golden-section bootstrap, by simulating independent zero-mean and unit-variance random variables, setting bootstrapped errors as $\widetilde{\mathbf{e}}^{*b}_{i,q}$ and $\widetilde{\mathbf{Y}}^{*b}_{i,q} := \widetilde{\mathbf{X}}_{i,\widetilde{p}}\widehat{\widetilde{\mathbf{B}}}^{(\lambda),C}_{\widetilde{p},q} + \widetilde{\mathbf{e}}^{*b}_{i,q}$, for each $i = 1, \ldots, n$ and $b = 1, \ldots, B$, being B the number of replicates.
5. After centering them, from the bootstrap sample, recompute the FPCR-L1S estimator in (4), obtaining the bootstrapped residuals and statistic $\mathrm{PCvM}^{*b}_{n,\widetilde{p},q}$ from (15).
6. Estimate the p-value as $\#\left\{\mathrm{PCvM}_{n,\widetilde{p},q} \leq \mathrm{PCvM}^{*b}_{n,\widetilde{p},q}\right\}/B$.

Remark 4. Note that the bootstrap procedure would provide sufficient guarantees if the residuals are perturbed (just until step 4 of Algorithm 1) without re-estimating the model (as done in step 5). The use of bootstrap for calibrating CvM and Kolmogorov-Smirnov (KS) statistics, in the context of functional time series (see Cao 1999 and Franke and Nyarige 2019), is supported by the consistency results demonstrated in the case of AR(1) processes (see Koul and Stute 1999). Since both the CvM statistic and the KS statistic are defined by a continuous functional, as well as the projection operator (which projects an ARH(1) onto a collection of AR(1) processes), the perturbed process has the same limiting distribution as the non-perturbed process (which, when projected, is the same as the one derived in Koul and Stute 1999). See also Chen et al. (2020) and alternatives bootstrap procedures in Shang (2018).

3.4. Numerical results: a comparative study

The performance of the test, regarding power and size, is now compared to the multi-stage testing procedure in Kokoszka and Reimherr (2013), abbreviated as **KR**, to determine the order of an ARH process. Note that their approach was developed just under ARH alternatives, in contrast with our unspecified alternatives. The following common settings will be used through scenarios described in Table 1: functional trajectories $\{\mathcal{X}_i\}_{i=1}^{n}$ and errors $\{\mathcal{E}_i\}_{i=1}^{n}$ (standard Brownian bridges), as shown in Fig. 1, are valued in 101 equispaced points in $[0, 1]$, with $\mathrm{M} = 1\,000$ Monte Carlo replicates, $\mathrm{B} = 1\,500$ bootstrap resamples. The initial values were simulated as standard Brownian bridges and a burn-in period of 200 functional observations was used. Our test was run following Algorithm 1, using initial cut-off levels (p, q) for ensuring us an explained variance of $\mathrm{EV}_p = \mathrm{EV}_q = 0.995$. Subsequently, the FPCR-L1S estimator in (4) was implemented by using the so-called one standard error rule λ_{1SE}, such that a L1-based variable selection is achieved. Note that, as discussed in Section 2 in the Supplementary Material, the variable selection is addressed focusing on the testing procedure, not on the estimation of the autocorrelation operator. Aimed at replicating all simulation studies, a companion R software is freely available at github.com/dadosdelaplace/gof-test-arh-ou-process. Concerning computational cost, one Monte Carlo iteration for our algorithm, fixed one data generation scenario and null hypothesis, for all sample sizes and all alternative hypotheses, it takes approximately 9 minutes. KS proposal it takes 1 minute approximately (but just for one of the alternative hypotheses). Computational times are all referred to a MacBook Pro computer (chip M2, 16Gb RAM, OS Ventura 13.4 and 250Gb flash disk).

The operator L in Table 1 is defined by $L(f) = \|f\|_{L^2([0,1]^2)}$ for each $f \in \mathbb{H}$. As summarized above, ARH(z) models are generated, with $z \in \{0, 1, 2\}$, and two nonlinear models, where $\rho(\mathcal{X})(\cdot) = \int_0^1 \beta(s, \cdot)\mathcal{X}(s)\mathrm{d}s$ and β are commonly kernels used in the literature (see Gabrys et al., 2010 and Hörmann and Kokoszka, 2010). In Table 1, $\mathcal{X}^2$ and $|\mathcal{X}|^{0.5}$ denote the pointwise exponentiation and

Table 1
Summary of null and alternative hypotheses.

Notation	Model	Parameters
ARH(0)	$\mathcal{X}_n(t) = \mathcal{E}_n(t)$	None
ARH(1)	$\mathcal{X}_n(t) = \rho_1(\mathcal{X}_{n-1})(t) + \mathcal{E}_n(t)$ $\beta_1(s,t) = c_1(2-(2s-1)^2-(2t-1)^2)$	$L(\beta_1) = 0.7$
ARH(2)	$\mathcal{X}_n(t) = \rho_1(\mathcal{X}_{n-1})(t) + \rho_2(\mathcal{X}_{n-2})(t) + \mathcal{E}_n(t)$ $\beta_i(s,t) = c_{2,i}e^{-(t^2+s^2)/2}$	$L(\beta_1) = 0.5$ $L(\beta_2) = 0.3$
Non linear, quadratic (**NLQ**)	$\mathcal{X}_n(t) = \rho_1\left(\mathcal{X}_{n-1}^2\right)(t) + \mathcal{E}_n(t)$ $\beta_1(s,t) = c_{2,1}e^{-(t^2+s^2)/2}$	$L(\beta_1) = 0.5$
Non linear, square root (**NLS**)	$\mathcal{X}_n(t) = \rho_1\left(\lvert\mathcal{X}_{n-1}\rvert^{0.5}\right)(t) + \mathcal{E}_n(t)$ $\beta_1(s,t) = c_{2,1}e^{-(t^2+s^2)/2}$	$L(\beta_1) = 0.5$

square root operations, respectively, to the discretized trajectories. Similar conditions on $L(\beta)$ proposed in Kokoszka and Reimherr (2013) are imposed, such that Assumptions 1–2 are held, and $(c_1, c_{2,1}, c_{2,2}) = (0.500568, 0.669502, 0.401701)$ are set. Table 2 shows the empirical rejection rates of testing $\mathcal{H}_0$ whether $\mathcal{X}_n$ is an ARH process of order z, with $z \in \{0,1,2\}$, comparing the performance of our proposed **CvM** test and the **KR** test, for scenarios in which data is generated following an ARH(z) model, with $z \in \{0,1,2\}$, and two nonlinear models. As remarked, the former test does not specify an alternative hypothesis, while the latter assumes a specific alternative (testing an ARH(z) against an ARH($z+1$) model). Nominal level $\alpha = 0.05$ and sample sizes $n \in \{150, 250, 350, 500, 750\}$, are considered (see Tables 2 and 3 in Supplementary Material about nominal levels $\alpha = 0.01$ and $\alpha = 0.1$).

The values presented in Table 2 (and in the subsequent tables) indicate the proportion of Monte Carlo replicates in which the null hypothesis is rejected. According to scenarios displayed in Table 2, regarding the size under null hypotheses, **CvM** and **KR** tests seem to be well calibrated, though both show a slight over-rejection in the ARH(1) scenario when indeed testing ARH(1) as $\mathcal{H}_0$. As observed, size of tests is also close to the nominal level $\alpha = 0.05$, even when small sample size is considered. Concerning powers under ARH alternatives, the **KR** test is more powerful, as expected since the **KR** test was specifically designed for these scenarios, rejecting ARH(z) in favor of ARH($z+1$). However, since **KR** test assumes an ARH structure even under alternatives, it fails against nonlinear alternatives, showing a poor power, in contrast with the high empirical power exhibits by our **CvM test** in most of scenarios. As opposed to the **KR** test, our proposal shows an increasing power inasmuch as increasing the sample size.

4. Stochastic differential equations: specification test

The methodology introduced in Section 3 can be further extended to diffusion processes, where the common framework is one dimensional, as usually one path of the process is considered. However, in finance, and motivated by the increasingly availability of high-frequency data, multivariate GoF tests could be unsuitable for such data, and thus, functional data setup has been exploited to take advantage of the shapes of curves (Müller et al., 2011). As a sideways contribution, a new specification test for diffusion models, from a high-dimensional data perspective, is now provided, namely for OU processes.

4.1. Diffusion models

As referred, stochastic diffusion models, as solutions to SDEs, have been increasingly used the last decades. From now on, given a filtered space $\left(\Omega, \{\mathcal{A}_t\}_{t\in[0,T]}, \mathbb{P}\right)$, associated to a probability space, the following parametric time-homogeneous one dimensional SDE is considered

$$\mathrm{d}\xi_t = m(\xi_t, \theta)\mathrm{d}t + \sigma(\xi_t, \theta)\mathrm{d}W_t, \quad t \in \mathbb{R}^+, \quad \{W_t\}_{t\in\mathbb{R}^+} \text{ a standard Wiener process}, \tag{17}$$

where $m: \mathbb{R}\times\mathbb{R}^d \to \mathbb{R}$ and $\sigma: \mathbb{R}\times\mathbb{R}^d \to \mathbb{R}^+$ are the drift and volatility functions, respectively, with $\theta \in \Theta \subset \mathbb{R}^d$. The diffusion model in (17) is commonly represented in its integral version, where ξ_t is $\mathcal{A}_t$-measurable, for each $t \in [0,T]$, as

$$\xi_t = \xi_0 + \int_0^T m(\xi_s, \theta)\mathrm{d}s + \int_0^T \sigma(\xi_s, \theta)\mathrm{d}W_s, \qquad \xi_0 \text{ initial condition at } t_0 = 0, \tag{18}$$

A strong solution of (18) is guaranteed under the boundedness, and Lipschitz and linear growth conditions (see, e.g., Karatzas and Shreve, 1998) on $m(\cdot)$ and $\sigma(\cdot)$:

Assumption 3 *(Global Lipschitz).* For all $x, y \in \mathbb{R}$, there exist $C_1 \in (0,\infty)$, not depending on parameters θ, such that $|m(x,\theta) - m(y,\theta)| + |\sigma(x,\theta) - \sigma(y,\theta)| \le C_1 |x-y|$.

Assumption 4 *(Linear growth).* For all $x \in \mathbb{R}$, there exist $C_2 \in (0,\infty)$, not depending on the set of parameters θ, such that $|m(x,\theta)| + |\sigma(x,\theta)| \le C_2 (1+|x|)$.

Table 2
Empirical size and power of **CvM** and **KR** tests for testing the ARH process order. Under $\mathcal{H}_0$, boldfaced rejection rates lie outside a 95%-confidence interval for $\alpha = 0.05$.

		CvM [unspecified $\mathcal{H}_1$]				
Data	$\mathcal{H}_0$	150	250	350	500	750
ARH(0)	ARH(0)	0.042	0.042	0.047	0.041	0.061
	ARH(1)	0.045	0.042	0.047	0.040	0.055
	ARH(2)	**0.031**	**0.029**	0.062	0.058	0.051
ARH(1)	ARH(0)	1.000	1.000	1.000	1.000	1.000
	ARH(1)	**0.030**	0.047	0.058	0.041	0.061
	ARH(2)	**0.189**	**0.117**	0.061	0.051	0.048
ARH(2)	ARH(0)	1.000	1.000	1.000	1.000	1.000
	ARH(1)	0.367	0.596	0.632	0.651	0.908
	ARH(2)	**0.011**	**0.027**	0.037	0.041	0.053
NLQ	ARH(0)	0.541	0.818	0.949	0.998	0.998
	ARH(1)	0.535	0.808	0.946	0.984	0.987
	ARH(2)	0.0462	0.791	0.931	0.948	0.972
NLS	ARH(0)	0.203	0.358	0.580	0.795	0.854
	ARH(1)	0.198	0.355	0.597	0.797	0.871
	ARH(2)	0.182	0.354	0.585	0.766	0.856

			KR				
Data	$\mathcal{H}_0$	$\mathcal{H}_1$	150	250	350	500	750
ARH(0)	ARH(0)	ARH(1)	0.045	0.056	0.051	0.054	0.059
	ARH(1)	ARH(2)	0.056	0.055	0.061	0.050	0.053
	ARH(2)	ARH(3)	**0.034**	0.043	0.049	0.060	0.057
ARH(1)	ARH(0)	ARH(1)	1.000	1.000	1.000	1.000	1.000
	ARH(1)	ARH(2)	0.056	0.053	0.063	0.042	0.055
	ARH(2)	ARH(3)	**0.031**	0.041	0.057	0.058	0.047
ARH(2)	ARH(0)	ARH(1)	1.000	1.000	1.000	1.000	1.000
	ARH(1)	ARH(2)	0.954	1.000	1.000	1.000	1.000
	ARH(2)	ARH(3)	0.040	0.043	0.059	0.057	0.053
NLQ	ARH(0)	ARH(1)	0.406	0.652	0.842	0.972	0.994
	ARH(1)	ARH(2)	0.059	0.047	0.058	0.048	0.067
	ARH(2)	ARH(3)	0.120	0.203	0.450	0.607	0.825
NLS	ARH(0)	ARH(1)	0.164	0.235	0.311	0.426	0.559
	ARH(1)	ARH(2)	0.056	0.045	0.069	0.053	0.098
	ARH(2)	ARH(3)	0.082	0.077	0.109	0.162	0.154

SDEs are usually discretely observed on a time interval $[0, T]$, discretized at equally spaced time points $\{t_0, t_1, \ldots, t_N\}$. In keeping with the Euler-Maruyama discretization scheme, SDE in (17) is approximated as $\xi_{t_{i+1}} - \xi_{t_i} \approx m\left(\xi_{t_i}, \theta\right)\Delta + \sigma\left(\xi_{t_i}, \theta\right)\sqrt{\Delta}\left(W_{t_{i+1}} - W_{t_i}\right)$, for each $i = 0, 1, \ldots, N-1$, where $\Delta = T/N$ is the length of the sampling intervals, and $\left\{\left(W_{t_{i+1}} - W_{t_i}\right)\right\}_{i=0}^{N-1}$ are iid zero-mean Gaussian random variables. Among the different specifications of (17), a common family of parametric models have been extensively used during the last decades, motivated by capturing the dynamics of the short-term interest rates (see, e.g., Vasicek 1977), which can be nested in the CKLS model (Chan et al., 1992),

$$\mathrm{d}\xi_t = \kappa(\mu - \xi_t)\mathrm{d}t + \sigma\xi_t^{\rho}\mathrm{d}W_t, \qquad t \in \mathbb{R}^+, \qquad \sigma > 0 \text{ (volatility around the mean)}, \tag{19}$$

where μ is the long term mean and $\kappa > 0$ is the speed of adjustment to μ (rate of mean reversion). A wide class of interest rate models can be obtained from (19), imposing restrictions to $(\mu, \kappa, \sigma, \rho)$, mainly epitomized by well-known the OU processes, with $\rho = 0$.

4.2. Ornstein-Uhlenbeck: a particular ARH(1) process

As referred, the relevance of OU processes is not limited to finance, since they have a long history in physics. This process, which constitutes a CKLS model in (19) with $\rho = 0$, and formalized as $\mathrm{d}\xi_t = \kappa(\mu - \xi_t)\mathrm{d}t + \sigma\mathrm{d}W_t$, with $t \in \mathbb{R}^+$, and $\kappa,\ \sigma > 0$, is often employed under its integral representation (via Fourier method of separation of variables), with $\kappa,\ \sigma > 0$:

$$\xi_t = \xi_0 e^{-\kappa t} + \mu\left(1 - e^{-\kappa t}\right) + \sigma\int_0^t e^{-\kappa(t-s)}\mathrm{d}W_s, \quad t \in \mathbb{R}^+,\ \xi_0 \text{ initial condition at } t_0 = 0. \tag{20}$$

With the same philosophy of the splitted representation adopted in Section 3 (see Fig. 1), and according to the proposal by Álvarez-Liébana et al. (2016), the OU process in (20) can be characterized as an ARH(1) process. Let $\mathbb{H}$ be a separable Hilbert space given by $\mathbb{H} = L^2\left([0,h], \mathcal{B}_{[0,h]}, \lambda + \delta_{(h)}\right)$, where $\mathcal{B}_{[0,h]}$ is the σ-algebra generated by subintervals $[0,h]$, λ denotes the Lebesgue measure and $\delta_{(h)}(s) = \delta(s-h)$ is the Dirac measure at h. The associated norm is defined as $\|\mathcal{X}\|_{\mathbb{H}} = \sqrt{\int_0^h \mathcal{X}^2(s)\mathrm{d}\left(\lambda + \delta_{(h)}\right)} = \sqrt{\int_0^h \mathcal{X}^2(s)\mathrm{d}s + \mathcal{X}^2(h)}$. Remark that $\|\cdot\|_{\mathbb{H}}$ directly establishes equivalent classes of functions such that $\mathcal{X} \sim_{\lambda+\delta_{(h)}} \mathcal{Y}$ if and only if $\lambda(\{s:\ \mathcal{X}(s) \neq \mathcal{Y}(s)\}) = 0$ and $\mathcal{X}(h) = \mathcal{Y}(h)$. In this setting, the OU process in (20) can be splitted as follows, for each $n \in \mathbb{Z}$:

$$\mathcal{X}_n(t) = \xi_{nh+t} = \xi_0 e^{-\kappa(nh+t)} + \mu\left(1 - e^{-\kappa(nh+t)}\right) + \sigma \int_0^{nh+t} e^{-\kappa(nh+t-s)}\mathrm{d}W_s, \qquad t \in [0,h],$$

and then, $e^{-\kappa t}\mathcal{X}_{n-1}(h) = e^{-\kappa t}\xi_{nh} = \xi_0 e^{-\kappa(nh+t)} + \mu\left(e^{-\kappa t} - e^{-\kappa(nh+t)}\right) + \sigma\int_0^{nh} e^{-\kappa(nh+t-s)}\mathrm{d}W_s$. The set of paths $\left\{\mathcal{X}_n(t)\right\}_{n\in\mathbb{Z}} = \left\{\xi_{nh+t}:\ t \in [0,h]\right\}_{n\in\mathbb{Z}}$ can be expressed as follows:

$$e^{-\kappa t}\left(\mathcal{X}_{n-1}(h) - \mu\right) = \left(\mathcal{X}_n(t) - \mu\right) - \sigma \int_{nh}^{nh+t} e^{-\kappa(nh+t-s)}\mathrm{d}W_s.$$

From now on, $\left\{\xi_t\right\}_{t\in\mathbb{R}^+}$ will be centered respect to its long term mean ($\mu = 0$), and, from Álvarez-Liébana et al. (2016), the OU process in (20) can be characterized as a zero-mean stationary ARH(1) process $\left\{\mathcal{X}_n(t) := \xi_{nh+t},\ t \in [0,h]\right\}_{n\in\mathbb{Z}}$ (see Fig. 1), given by

$$\mathcal{X}_n(t) = e^{-\kappa t}\mathcal{X}_{n-1}(h) + \sigma \int_{nh}^{nh+t} e^{-\kappa(nh+t-s)}\mathrm{d}W_s = \rho_\kappa\left(\mathcal{X}_{n-1}\right)(t) + \mathcal{E}_n(t), \qquad n \in \mathbb{Z}, \tag{21}$$

where $\left\{\mathcal{E}_n(t) := \sigma\int_{nh}^{nh+t} e^{-\kappa(nh+t-s)}\mathrm{d}W_s\right\}_{n\in\mathbb{Z}}$ constitutes a $\mathbb{H}$-valued strong white noise and ρ_κ is a bounded linear operator, for each $\kappa > 0$ (Álvarez-Liébana et al., 2016). Note the reader that $\left\|\rho_\kappa(\mathcal{X})\right\|_{\mathbb{H}}^2 = \int_0^h \left|\rho_\kappa(\mathcal{X})(t)\right|^2 \mathrm{d}t + \left|\rho_\kappa(\mathcal{X})(h)\right|^2$, for each $\mathcal{X} \in \mathbb{H}$, $\left\|\rho_\kappa^k\right\|_{\mathcal{L}(\mathbb{H})} < 1$, for each $k \geq k_0$ and for some $k_0 \geq 1$ (Álvarez-Liébana et al., 2016, Lemma 1).

4.3. A two-steps specification test for the OU model

As explained, the ARH(1) characterization of an OU process provided in (21) will allow us to propose a two-stage methodology in this subsection with the aim of developing a specification test for these diffusion processes. In brief, the underlying idea will be, firstly, test whether a diffusion process $\left\{\xi_t\right\}_{t\in\mathbb{R}^+}$, splitted and characterized as $\left\{\mathcal{X}_n(t) := \xi_{nh+t},\ t \in [0,h]\right\}_{n\in\mathbb{Z}}$, constitutes an ARH(1) process (via Algorithm 1), i.e., testing whether, for each $n \in \mathbb{Z}$,

$$\mathcal{H}_0^{(1)}:\ \mathcal{X}_n \text{ and } \mathcal{X}_{n-1} \text{ are linearly related via } \rho \in \mathcal{L}, \qquad \mathcal{X}_n(t) = \rho\left(\mathcal{X}_{n-1}\right)(t) + \mathcal{E}_n(t). \tag{22}$$

After the characterization of an ARH(1) process as a FLMFR model in (14), the second stage will be to check the parametric form of the linear operator ρ, with the null hypothesis $\mathcal{H}_0^{(2)}:\ \rho(\mathcal{X})(t) := \rho_\kappa(\mathcal{X})(t) = e^{-\kappa t}\mathcal{X}(h)$, for each $\mathcal{X} \in \mathbb{H} = L^2\left([0,h], \mathcal{B}_{[0,h]}, \lambda + \delta_{(h)}\right)$ ($\mathcal{X}_n(t) = \xi_{nh+t} = \xi_0 e^{-\kappa(nh+t)} + \sigma\int_0^{nh+t} e^{-\kappa(nh+t-s)}\mathrm{d}W_s$, for each $n \in \mathbb{Z}$), via a functional F-test, as long as the linear null hypothesis $\mathcal{H}_0^{(1)}$ in (22) is not rejected, against the alternative of an unspecified FLMFR.

As referred, a F-test will be implemented. In keeping with the classical F-statistic, the functional version proposed by Shen and Faraway (2004) has been implemented, based on the residual sum of squared norm (RSSN) of functional errors (Cuevas et al., 2004):

$$\mathrm{RSSN}_n = \sum_{i=0}^{n-1} \left\|\mathcal{Y}_i - \hat{\mathcal{Y}}_i\right\|_{\mathbb{H}}^2, \qquad \mathcal{Y}_i = \rho\left(\mathcal{X}_i\right) + \mathcal{E}_i, \qquad F_n = \frac{\mathrm{RSSN}_n^{\mathrm{OU}} - \mathrm{RSSN}_n^{\mathrm{FLMFR}}}{\mathrm{RSSN}_n^{\mathrm{FLMFR}}}, \tag{23}$$

where $\mathrm{RSSN}_n^{\mathrm{OU}}$ denotes the RSSN of functional errors under the assumption that the linear operator is parametric defined as $\rho(\mathcal{X})(t) := \rho_\kappa(\mathcal{X})(t) = e^{-\kappa t}\mathcal{X}(h)$ (i.e., under null hypothesis $\mathcal{H}_0^{(2)}$), whereas $\mathrm{RSSN}_n^{\mathrm{FLMFR}}$ denotes the RSSN of functional errors of an unrestricted FLMFR, whose estimator is given by the FPCR-L1S estimator provided in Section 2.1. In the former case, and estimator of $\rho_\kappa(\mathcal{X})(t) = e^{-\kappa t}\mathcal{X}(h)$ is required, in terms of the maximum likelihood sample-dependent estimator $\hat{\kappa}_n = \frac{-\int_0^{nh}\xi_t \mathrm{d}\xi_t}{\int_0^{nh}\xi_t^2\mathrm{d}t}$ proposed in Álvarez-Liébana et al. (2016), whose strong-consistency was therein proved. Henceforth, $\hat{\rho}_\kappa(\mathcal{X})(t) := \rho_{\hat{\kappa}_n}(\mathcal{X})(t) = e^{-\hat{\kappa}_n t}\mathcal{X}(h)$ is considered. In Algorithm 2, a summary of the testing procedure is presented, via Bonferroni correction to counteract the multiple tests.

Algorithm 2. Let $\left\{\xi_t\right\}_{t\in[0,T]}$ be stochastic processes on a given filtered space $\left(\Omega, \left\{\mathcal{A}_t\right\}, \mathbb{P}\right)$ where ξ_t is $\mathcal{A}_t$-measurable, for each $t \in [0,T]$, given by a parametric time-homogeneous SDE (see (17)), under Assumptions 3–4 and long term mean μ equal to zero. It proceeds as follows:

Stage 1 ($\mathcal{H}_0^{(1)}$): testing if $\left\{\xi_t\right\}_{t\in[0,T]}$ can be reinterpreted as a functional ARH(1) model.

1. Split $\{\xi_t\}_{t\in[0,T]}$ into a set of functional paths $\{\mathcal{X}_i(t) := \xi_{ih+t},\ t\in[0,h]\}_{i=0}^{n-1}$ valued in n subintervals, where $T = nh$ and $\mathcal{X}_i \in L^2\left([0,h], \mathcal{B}_{[0,h]}, \lambda + \delta_{(h)}\right)$. Without loss of generality, $h = 1$, since for curves evaluated in $[a,b]$, a simple translation can be performed using the transformation $g(t) := f((t-a)/(b-a))$, where f is evaluated on $[0,1]$ and g on $[a,b]$.
2. Construct frv's $\widetilde{\mathcal{X}}_i(s) := \mathcal{X}_{i-1}(s)$, $\widetilde{\mathcal{Y}}_i(t) := \mathcal{X}_i(t)$ and $\widetilde{\mathcal{E}}_i(t) := \mathcal{E}_i(t)$, all of them centered, with $\widetilde{\mathcal{Y}}_i = \widetilde{\rho}\left(\widetilde{\mathcal{X}}_i\right) + \widetilde{\mathcal{E}}_i$, for any $i = 1,\dots,n-1$, and $s,t\in[0,h]$.
3. Obtain the FPC of $\left\{\widetilde{\mathcal{X}}_i\right\}_{i=1}^{n-1}$ and $\left\{\widetilde{\mathcal{Y}}_i\right\}_{i=1}^{n-1}$, choose initial (p,q) required for $\mathrm{EV}_p = \mathrm{EV}_q = 0.99$, and achieve their p- and q-truncated FPC scores $\widetilde{\mathbf{X}}_p$ and $\widetilde{\mathbf{Y}}_q$, respectively. The FPCR-L1S estimator $\widehat{\widetilde{\mathbf{B}}}_{\widetilde{p},q}^{(\lambda),C}$ is then computed, and the associated residuals. As detailed in Algorithm 1, the statistic $\mathrm{PCvM}_{n,\widetilde{p},q}$ in (15) is computed, the bootstrapped errors $\left\{\mathbf{e}_{i,q}^{*b}\right\}_{i=1,\dots,n-1}^{b=1,\dots,B}$, whit B replicates, and the bootstrapped statistic $\mathrm{PCvM}_{n,\widetilde{p},q}^{*b}$.
4. Estimate the p-value as $p^{(1)} := \#\left\{\mathrm{PCvM}_{n,\widetilde{p},q} \le \mathrm{PCvM}_{n,\widetilde{p},q}^{*b}\right\}/B$. If $\mathcal{H}_0^{(1)}$ in (22) is rejected, the procedure stops. Otherwise, go to stage 2.

Stage 2 ($\mathcal{H}_0^{(2)}$): testing if $\{\xi_t\}_{t\in[0,T]}$, characterized as an ARH(1) model (under linearity), constitutes an OU process via F-test, against the alternative of an unspecified FLMFR.

5. If $\mathcal{H}_0^{(1)}$ in (22) is not rejected, calculate the F-statistic as $F_n = \frac{\mathrm{RSSN}_n^{\mathrm{OU}} - \mathrm{RSSN}_n^{\mathrm{FLMFR}}}{\mathrm{RSSN}_n^{\mathrm{FLMFR}}}$, where RSSN_n is computed as (23), with $\mathrm{RSSN}_n^{\mathrm{OU}} = \sum_{i=1}^{n-1}\left\|\widetilde{\mathcal{Y}}_i(t) - e^{-\hat{\kappa}_n t}\widetilde{\mathcal{X}}_i(h)\right\|_{\mathbb{H}}^2$.
6. A parametric bootstrap is implemented, by simulating a set of OU processes $\{\xi_t^{*b}\}_{t\in[0,T]}^{b=1,\dots,B}$, driven by $\mathrm{d}\xi_t^{*b} = -\hat{\kappa}_n\xi_t^{*b}\mathrm{d}t + \hat{\sigma}_n\mathrm{d}W_t^{*b}$, for each $b = 1,\dots,B$, where B is the number of replicates, $\hat{\sigma}_n = \arg\min_{\sigma_0}\frac{1}{N-1}\sum_{i=0}^{N-1}\left(\ln\left(\sigma_0^2\right) + \frac{\left(\xi_{t_{i+1}} - \xi_{t_i}\right)^2}{\sigma_0^2\Delta}\right)$ is the consistent estimator of σ (Corradi and White, 1999) and $\hat{\kappa}_n$ is the referred estimator of κ, where $\{t_0,\dots,t_N\}$ are the grid points of $[0,T]$, with $T = nh$, and Δ the discretization step.
7. With the bootstrapped $\{\xi_t^{*b}\}_{t\in[0,T]}^{b=1,\dots,B}$, $F_n^{*b} = \frac{\mathrm{RSSN}_n^{OU,*b} - \mathrm{RSSN}_n^{FLMFR,*b}}{\mathrm{RSSN}_n^{FLMFR,*b}}$ is recomputed, such that an estimator $\hat{\kappa}_n^{*b}$ is required to be recomputed, as well as a FPCR-L1S estimator for $\rho_{\hat{\kappa}_n}$, for each $b = 1,\dots,B$.
8. Estimate the p-value as $p^{(2)} := \#\left\{F_n \le F_n^{*b}\right\}/B$.

Bonferroni correction: stage 1 + stage 2. As multiple tests are conducting, given the corresponding p-values $p^{(1)}$ and $p^{(2)}$ for testing the hypotheses $\mathcal{H}_0^{(1)}$ and $\mathcal{H}_0^{(2)}$, the Bonferroni correction is used to set an upper bound on the significance level α (Miller, 1981), by rejecting $\mathcal{H}_0 = \{\mathcal{H}_0^{(1)}, \mathcal{H}_0^{(2)}\}$ if any p-value $p^{(1)}$ or $p^{(2)}$ is less than $\alpha/2$. As referred, the second stage in Algorithm 2 is omitted if $\mathcal{H}_0^{(1)}$ is rejected, respect to $\alpha/2$.

4.4. Simulation study

The finite sample properties of the specification test are illustrated with 1 000 Monte Carlo replicates and $B = 1\,000$ bootstrap resamples, with $n\in\{50,150,250,350,500,1000,5000\}$, such that trajectories $\left\{\mathcal{X}_i(t) := \xi_{ih+t}\right\}_{i=0}^{n-1}$ are valued in 101 equispaced points in $[0,1]$. The FPCR-L1S estimator was used with $\mathrm{EV}_p = \mathrm{EV}_q = 0.995$. As reflected in Table 3, several scenarios have been simulated. Under $\mathcal{H}_0$, sample paths are simulated for the centered OU model in (20). On the other hand, concerning the power, different interest rate models are simulated, as the CKLS model (Chan et al., 1992), the Inverse Feller (IF) model (Ahn and Gao, 1999) and the Aït-Sahalia (AS) model (Aït-Sahalia, 1996). Similar parameters of the CKLS model to those ones proposed in Hong and Li (2004), to examine different persistent dependence and volatility, were tested. The IF and AS models are given by $\mathrm{d}\xi_t = \xi_t(\kappa - (\sigma^2 - \kappa\mu)\xi_t)\mathrm{d}t + \sigma\xi_t^{3/2}\mathrm{d}W_t$ and $\mathrm{d}\xi_t = (\tau_{-1}\xi_t^{-1} + \tau_0 + \tau_1\xi_t + \tau_2\xi_t^2)\mathrm{d}t + \sigma\xi_t^{3/2}\mathrm{d}W_t$, with similar set of parameters as proposed in Ahn and Gao (1999) and Aït-Sahalia (2001), respectively (see Table 3). For testing deviations from the null hypothesis, the radial OU process is also considered, given by $\mathrm{d}\xi_t = (\lambda\xi_t^{-1} - \kappa\xi_t)\mathrm{d}t + \sigma\mathrm{d}W_t$, which corresponds with the OU if $\lambda = 0$. Note that the drift function is non-Lipschitz and unbounded, however, there exists a unique weak SDE solution. A null model has been also tested, given by $\mathrm{d}\xi_t = \sigma\mathrm{d}W_t$, with $\sigma\in\{0.1,0.5\}$.

Table 4 displays the empirical sizes and powers, respectively, with $\alpha = 0.05$ as nominal level. In the former table, regarding the calibration of test, the empirical sizes are close to α through all values of σ and κ. As expected, scenarios with $n = 50$ exhibit over-rejection for larger κ values, owing to κ represents the speed of reversion at which trajectories are rearranged around μ, and then, greater values of κ lead to more similar paths to be discriminated, since $\lim_{t\to\infty}\mathrm{Var}\left[\xi_t\right] = \frac{\sigma^2}{2\kappa}$ constitutes the long term variance. This behavior is overcome as n increases: just 2 of the 90 scenarios (2.22% of cases) with $n\in\{150,250,350,500,1000,5000\}$ display slightly over-rejections (boldfaced rejection rates). Note that sample size in the functional data framework refers to the number of

Table 3
Summary of simulated scenarios.

Notation	Description	Model	Parameters and scenarios
$\mathcal{H}_0$	OU (centered)	$\mathrm{d}\xi_t = -\kappa\xi_t\mathrm{d}t + \sigma\mathrm{d}W_t$	$\kappa \in \{0.2, 0.5, 0.8\}$ $\sigma^2 \in \{0.008, 0.05, 0.15, 0.50, 0.75\}$
$\mathcal{H}_{1,Null}$	Null	$\mathrm{d}\xi_t = \sigma\mathrm{d}W_t$	S1: $\sigma = 0.1$ S2: $\sigma = 0.5$
$\mathcal{H}_{1,IF}$	Inverse-Feller	$\mathrm{d}\xi_t = \xi_t(\kappa - (\sigma^2 - \kappa\mu)\xi_t)\mathrm{d}t + \sigma\xi_t^{3/2}\mathrm{d}W_t$	$(\kappa, \mu, \sigma^2) = (0.364, 0.08, 1.6384)$
$\mathcal{H}_{1,AS}$	Aït-Sahalia	$\mathrm{d}\xi_t = (\tau_{-1}\xi_t^{-1} + \tau_0 + \tau_1\xi_t + \tau_2\xi_t^2)\mathrm{d}t + \sigma\xi_t^{3/2}\mathrm{d}W_t$	$(\tau_{-1}, \tau_0, \tau_1, \tau_2, \sigma) = (0.00107, -0.0517\ 0.877, -4.604, 0.8)$
$\mathcal{H}_{1,CKLS}$	CKLS	$\mathrm{d}\xi_t = \kappa(\mu - \xi_t)\mathrm{d}t + \sigma\xi_t^{\rho}\mathrm{d}W_t$	S1: $(\mu, \kappa, \sigma, \rho) = (0.09, 0.9, 0.5, 1.5)$ S2: $(\mu, \kappa, \sigma, \rho) = (0.09, 0.2, 1.5, 1.5)$ S3: $(\mu, \kappa, \sigma, \rho) = (0.09, 0.2, 3, 1.5)$
$\mathcal{H}_{1,ROU}$	Radial OU	$\mathrm{d}\xi_t = (\lambda\xi_t^{-1} - \kappa\xi_t)\mathrm{d}t + \sigma\mathrm{d}W_t$	S1: $(\lambda, \kappa, \sigma) = (0.05, 0.1, 0.5)$ S2: $(\lambda, \kappa, \sigma) = (0.075, 0.1, 0.5)$ S3: $(\lambda, \kappa, \sigma) = (0.1, 0.1, 0.5)$ S4: $(\lambda, \kappa, \sigma) = (0.125, 0.1, 0.5)$

curves, the actual number of observations in the simulation reaches 500 000 for the $n = 5\,000$ scenario, as the curves are evaluated in 101 equispaced points.

With respect to empirical power (Table 4b), deviations from the null, by augmenting λ in the radial OU, show the increasing power of the test as n increases. The null model also exhibits high empirical powers, just like the nonlinear drift alternatives, specially the IF model, displaying great empirical powers even for small sample sizes. Concerning the CKLS model, all the scenarios provide increasing rejection rates, such that the higher the volatility parameter, the more empirical power. A slightly poor performance is empirically obtained for the more complex AS model, although empirical powers seem to tend to one as n increases. This apparent lower performance may be attributed, in all likelihood, to the model's greater inclusion of nonlinear terms, thereby resulting in a greater 'distance' from the model assumed in the null hypothesis.

5. Real data applications

Motivated by the extensive use of diffusion processes in finance, commonly used to model currency exchange rates (Ball and Roma, 1994) and intra-day patterns in the foreign exchange market (Andersen and Bollerslev, 1997), it is illustrated a real-data application of our OU specification test, in the context of high-frequency financial data. Unlike univariate frameworks, where a vast time window is required for getting properly sample sizes, and thus, certain properties essential for long horizon asymptotics (e.g., ergodicity) would not be achieved, a finite time observation window is considered, where the functional data scheme allows to capture the dynamic of the process (Müller et al., 2011).

The three datasets considered consist on currency pair rates Euro-British pound (EURGBP), Euro-US Dollar (EURUSD), British pound-US Dollar (GBPUSD), determined in the foreign exchange market, such that data was recorded every 5 minutes from January 1, 2019 to December 31, 2019, and they are freely available in https://github.com/dadosdelaplace/gof-test-arh-ou-process. Fig. 2 shows the exchange rates (top) with 73 440 observations, and the splitted paths (bottom) $\{\mathcal{X}_i(t)\}_{i=1}^n$ featuring $n = 255$ daily curves. The daily curves are valued in $\mathbb{H} = L^2\left([0,1], \mathcal{B}_{[0,1]}, \lambda + \delta_{(1)}\right)$, where the interval $[0,1]$ accounts for a 1-day window, discretized in 288 equispaced grid points. Table 5 shows the empirical p-values for the three datasets, with $B = 1\,000$ bootstrap resamples, at each of the two-stages defined in Algorithm 2. In this way, it is tested at stage one the null hypothesis that the daily curves $\{\mathcal{X}_i(t)\}_{i=1}^n$ constitute an ARH(1) process,

$$\mathcal{H}_0^{(1)}: \ \mathcal{X}_n \text{ and } \mathcal{X}_{n-1} \text{ are linearly related via } \rho \in \mathcal{L},$$

with $\mathcal{X}_n(t) = \rho\left(\mathcal{X}_{n-1}\right)(t) + \mathcal{E}_n(t)$. At stage two, a F-test is implemented to test the parametric form of the OU process, $\mathcal{H}_0^{(2)}: \ \rho(\mathcal{X})(t) := \rho_\kappa(\mathcal{X})(t) = e^{-\kappa t}\mathcal{X}(h)$.

Regarding the p-values from Table 5, the null hypothesis of OU process in the EURGBP series is rejected, at a 5% level, since it does not seem to follow an stationary ARH(1) process (stage one) when the annual trajectory is considered as daily curves. However, it is not rejected for the EURUSD and GBPUSD exchange rates, where a simple model with constant volatility function as the OU seems to capture the dependence of the series. The nature of the sampling mechanism could generate a different result, as classical data analysis for diffusion processes deals with monthly, weekly or daily data, at most. As the sampling frequency is not dictated by the data, usually a large fraction of data is discarded, not without loss of information. In our data example, sampling daily would mean to retain only 255 observations, from a total of 73 440, working with one observation a day instead of the whole daily trajectory. Therefore, when dealing with intra-day data, conducting the study using a functional framework takes advantage of the information retained in the shape of the curve, treating the daily curves as a statistical object, instead of a collection of individual observations.

Table 4
(a) Empirical rejection rates under the null hypothesis (data is generated by different OU processes). The rejection rates are boldfaced if they lie outside a 95%-confidence interval for $\alpha = 0.05$. (b) Empirical rejection rates under the alternative hypothesis, from scenarios displayed in Table 3.

(a) Size simulation.

		n						
σ^2	κ	50	150	250	350	500	1000	5000
0.008	0.2	0.048	0.043	0.049	0.053	0.045	0.051	0.058
	0.5	0.047	0.053	0.048	0.046	0.050	0.049	0.052
	0.8	**0.078**	0.048	0.051	0.056	0.042	0.058	0.054
0.05	0.2	0.043	0.051	0.054	0.048	0.053	0.052	0.061
	0.5	0.051	0.057	0.055	0.055	0.061	0.048	0.054
	0.8	**0.102**	0.060	0.052	**0.075**	0.057	0.053	0.044
0.15	0.2	0.050	0.045	0.048	0.053	0.046	0.051	0.060
	0.5	0.045	0.053	0.053	0.046	0.050	0.050	0.048
	0.8	**0.078**	0.051	0.052	0.056	0.043	0.056	0.056
0.50	0.2	0.051	0.046	0.053	0.046	0.051	0.052	0.058
	0.5	0.050	0.056	0.059	0.054	0.053	0.051	0.061
	0.8	**0.096**	**0.065**	0.057	0.059	0.056	0.059	0.053
0.75	0.2	0.046	0.044	0.049	0.052	0.047	0.051	0.053
	0.5	0.048	0.054	0.050	0.047	0.051	0.048	0.052
	0.8	**0.080**	0.058	0.053	0.054	0.041	0.057	0.050

(b) Power simulation.

	n						
Scenario	50	150	250	350	500	1000	5000
$\mathcal{H}^{S1}_{1,ROU}$	0.043	0.145	0.241	0.340	0.481	0.818	0.945
$\mathcal{H}^{S2}_{1,ROU}$	0.060	0.232	0.390	0.530	0.744	0.956	0.989
$\mathcal{H}^{S3}_{1,ROU}$	0.070	0.280	0.487	0.722	0.900	0.976	1.000
$\mathcal{H}^{S4}_{1,ROU}$	0.065	0.276	0.586	0.807	0.945	0.986	1.000
$\mathcal{H}^{S1}_{1,Null}$	0.097	0.322	0.583	0.741	0.907	1.000	1.000
$\mathcal{H}^{S2}_{1,Null}$	0.108	0.317	0.566	0.765	0.919	1.000	1.000
$\mathcal{H}_{1,IF}$	0.455	0.750	0.836	0.870	0.928	0.976	1.000
$\mathcal{H}_{1,AS}$	0.139	0.370	0.499	0.611	0.756	0.958	1.000
$\mathcal{H}^{S1}_{1,CKLS}$	0.179	0.277	0.360	0.488	0.667	0.763	0.886
$\mathcal{H}^{S2}_{1,CKLS}$	0.319	0.635	0.727	0.738	0.811	0.895	0.994
$\mathcal{H}^{S3}_{1,CKLS}$	0.690	0.933	0.985	0.993	1.000	1.000	1.000

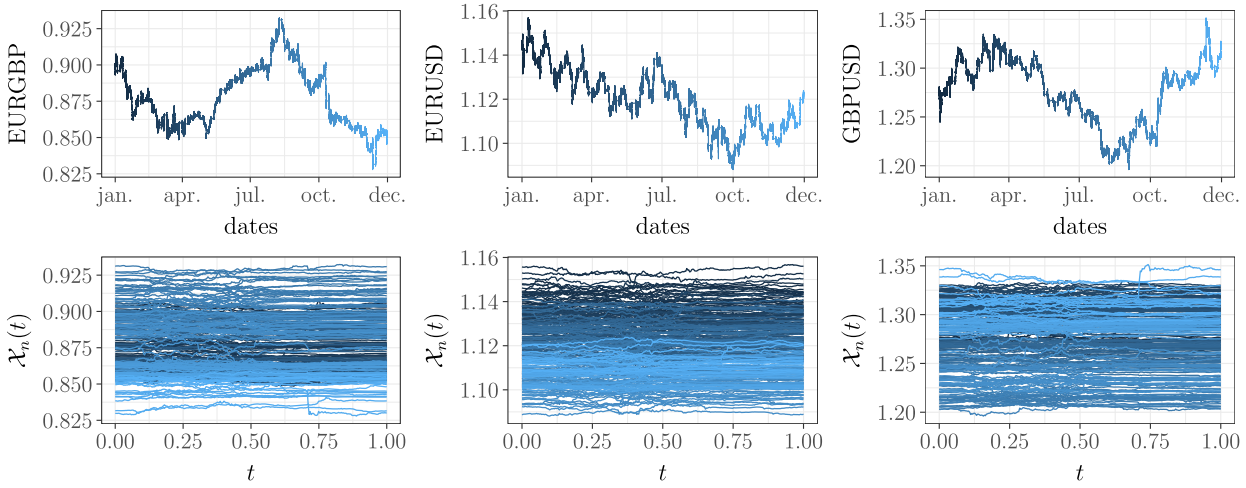

Fig. 2. From left to right: EURGBP, EURUSD and GBPUSD exchange rates throughout 2019. On the top, the observed stochastic process; at the bottom, daily splitted paths.

Table 5
p-values under the null hypothesis that series follows a centered OU process.

Two-stages test	EURGBP	EURUSD	GBPUSD
Stage 1: ARH(1) GoF test	0.020	0.339	0.091
Stage 2: F-test	0.349	0.253	0.510

6. Conclusions and discussion

In conclusion, a novel goodness-of-fit (GoF) test for ARH(z) models was proposed, against an unspecified alternative, based on their characterization as FLMFR. No competitors were identified against an unrestricted alternative; however, empirical results under various alternatives were compared with those of Kokoszka and Reimherr (2013) (KR) in determining the order z. The findings demonstrated that the proposed test is well-calibrated under the null hypothesis and exhibits strong power across several alternative scenarios, remaining competitive even against nonlinear alternatives where the KR test lacks sufficient power.

As noted, the current proposal is founded on the assumption that the functional data involved can be represented on an equally spaced grid, a common assumption in the context of diffusion processes. In instances where curves are available on an irregular grid, a substantial modification would involve first approximating their functional basis to a higher-resolution uniformly spaced grid. Subsequently, a sufficient number of points can be selected to minimize the compromise in the quality of the representation. This regularized process can be easily achieved using the functions provided by R package fda.usc. Concerning grid resolution, the regularity dotted by a Hilbert structure ensures that a sparse grid does not distort the representation (in terms of FPC) of our data, thereby avoiding a significant loss in estimation precision.

Additionally, a novel specification test for the Vasicek model was proposed, first characterizing it as an ARH(1) model, and secondly, testing the parametric form, under linearity, via a functional F-test, calibrated by a parametric bootstrap. The finite sample behavior was also illustrated, generating the data under parametric families of diffusion processes, providing the empirical evidence that the two-stage specification test is well-calibrated, and detected different alternative models widely used in finance. Traditional data analysis often overlooks the information contained in the shape of daily curves; thus, a functional data approach may be more suitable when dealing with intraday or high-frequency data, as it can extract additional information from the curves. The classical diffusion process framework regards the whole observation sequence as a single sample path, ignoring the process's patterns across days. In a functional data setting, one can leverage the information retained in the shape of the curve, treating daily curves as statistical objects rather than mere collections of individual observations. Results were illustrated through an application to daily currency exchange rate curves with 5-minute intervals, where the Vasicek model effectively captures the underlying dynamic changes in the daily curves for the EUR/USD and GBP/USD pairs.

Since lower-order autoregressive processes can be considered nested models within higher-order processes, the GoF test with composite hypotheses raised in the earlier sections does not distinguish whether an overparameterization has occurred (for example, if the process has been generated under an ARH(1) model, it will never reject a null hypothesis of ARH(z) with $z \geq 1$). This can be detected by modifying the methodology of Algorithm 2 to first conduct a general step assessing whether it falls within the ARH(z) models, followed by a specific specification test on its parametric form (and particularly its order).

Future applications may be developed, as the specification test discussed could be extended to other diffusion processes that can be characterized as ARH(z) models. If other diffusion processes in the literature can be characterized as ARH(z) (for instance, ARH(2)), the same methodology could be applied. The derived tests may also be extended to Hilbertian moving-average processes and ARH processes with exogenous variables. Ongoing work is focused on developing a fully functional procedure, as well as on the theoretical formulation of the asymptotic distribution of the statistic.

Acknowledgements

The authors gratefully thank Spanish National Research Council for the computing resources of the Supercomputing Center of Galicia (CESGA), and full professor M. D. Ruiz-Medina (University of Granada) for her suggestions. The first author acknowledges support from grants PID2020-116587GB-I00 and PGC2018-099549-B-I00, from the Spanish Ministry of Economy and Competitiveness. The second, third and fourth authors acknowledge financial support from grant PID2020-116587GB-I00 also from the same agency.

Appendix A. Supplementary material

Supplementary material related to this article can be found online at https://doi.org/10.1016/j.csda.2024.108092.

Software

A companion R software, allowing to replicate all tests and applications, is freely available at github.com/dadosdelaplace/gof-test-arh-ou-process, including real datasets here tested.

References

Ahn, D.H., Gao, B., 1999. A parametric nonlinear model of term structure dynamics. Rev. Financ. Stud. 12 (4), 721–762.

Aït-Sahalia, Y., 1996. Testing continuous-time models of the spot interest rate. Rev. Financ. Stud. 9 (2), 385–426.

Aït-Sahalia, Y., 2001. Transition densities for interest rate and other nonlinear diffusions. In: Quantitative Analysis in Financial Markets: Collected Papers of the New York University Mathematical Finance Seminar (Volume II).

Aït-Sahalia, Y., Fan, J., Peng, H., 2009. Nonparametric transition-based tests for jump diffusions. J. Am. Stat. Assoc. 104 (487), 1102–1116.

Álvarez-Liébana, J., Bosq, D., Ruiz-Medina, M.D., 2016. Consistency of the plug-in functional predictor of the Ornstein–Uhlenbeck process in Hilbert and Banach spaces. Stat. Probab. Lett. 117, 12–22.

Álvarez-Liébana, J., Bosq, D., Ruiz-Medina, M.D., 2017. Asymptotic properties of a component-wise ARH(1) plug-in predictor. J. Multivar. Anal. 155, 12–34.

Andersen, T.G., Bollerslev, T., 1997. Intraday periodicity and volatility persistence in financial markets. J. Empir. Finance 4 (2), 115–158.

Aneiros, G., Vieu, P., 2014. Variable selection in infinite-dimensional problems. Stat. Probab. Lett. 94, 12–20.

Arapis, M., Gao, J., 2006. Empirical comparisons in short-term interest rate models using nonparametric methods. J. Financ. Econ. 4 (2), 310–345.

Bagchi, P., Characiejus, V., Dette, H., 2018. A simple test for white noise in functional time series. J. Time Ser. Anal. 39 (1), 54–74.

Ball, C., Roma, A., 1994. Target zone modelling and estimation for European Monetary System exchange rates. J. Empir. Finance 1 (3), 385–420.

Berkes, I., Gabrys, R., Horváth, L., Kokoszka, P., 2009. Detecting changes in the mean of functional observations. J. R. Stat. Soc. B 71 (5), 927–946.

Bosq, D., 2000. Linear Processes in Function Spaces. Lecture Notes in Statistics. Springer, New York.

Cao, R., 1999. An overview of bootstrap methods for estimating and predicting in time series. Test 8, 95–116.

Chan, K.C., Karolyi, G.A., Longstaff, F.A., Sanders, A.B., 1992. An empirical comparison of alternative models of the short-term interest rate. J. Finance 47 (3), 1209–1227.

Chen, B., Hong, Y., 2010. Characteristic function–based testing for multifactor continuous-time Markov models via nonparametric regression. Econom. Theory 26 (4), 1115–1179.

Chen, F., Jiang, Q., Feng, Z., Zhu, L., 2020. Model checks for functional linear regression models based on projected empirical processes. Comput. Stat. Data Anal. 144, 106897.

Chen, Q., Zheng, X., Pan, Z., 2015. Asymptotically distribution-free tests for the volatility function of a diffusion. J. Econom. 184 (1), 124–144.

Chen, S.X., Gao, J., 2011. Simultaneous specification testing of mean and variance structures in nonlinear time series regression. Econom. Theory 27 (4), 792–843.

Chen, S.X., Gao, J., Tang, C.Y., 2008. A test for model specification of diffusion processes. Ann. Stat. 36 (1), 167–198.

Corradi, V., Swanson, N.R., 2005. Bootstrap specification tests for diffusion processes. J. Econom. 124 (1), 117–148.

Corradi, V., White, H., 1999. Specification tests for the variance of a diffusion. J. Time Ser. Anal. 20 (3), 253–270.

Cuesta-Albertos, J.A., García-Portugués, E., Febrero-Bande, M., González-Manteiga, W., 2019. Smoothing splines estimators for functional linear regression. Ann. Stat. 47 (1), 439–467.

Cuevas, A., Febrero-Bande, M., Fraiman, R., 2004. An ANOVA test for functional data. Comput. Stat. Data Anal. 47 (1), 111–122.

Dette, H., Podolskij, M., 2008. Testing the parametric form of the volatility in continuous time diffusion models: a stochastic process approach. J. Econom. 143 (1), 56–73.

Dette, H., von Lieres und Wilkau, C., 2003. On a test for a parametric form of volatility in continuous time financial models. Finance Stoch. 7 (3), 363–384.

Escanciano, J.C., 2006. A consistent diagnostic test for regression models using projections. Econom. Theory 2 (6), 1030–1051.

Fan, J., Zhang, C., 2003. A reexamination of diffusion estimators with applications to financial model validation. J. Am. Stat. Assoc. 98 (461), 118–134.

Fan, J., Jiang, J., Zhang, C., Zhou, Z., 2003. Time-dependent diffusion models for term structure dynamics. Stat. Sin. 13 (4), 965–992.

Franke, J., Nyarige, E.G., 2019. A residual-based bootstrap for functional autoregressions. arXiv:1905.07635.

Friedman, J., Hastie, T., Tibshirani, R., 2010. Regularization paths for Generalized Linear Models via coordinate descent. J. Stat. Softw. 33 (1), 1–22.

Gabrys, R., Kokoszka, P., 2007. Portmanteau test of independence for functional observations. J. Am. Stat. Assoc. 102 (480), 1338–1348.

Gabrys, R., Horváth, L., Kokoszka, P., 2010. Tests for error correlation in the functional linear model. J. Am. Stat. Assoc. 105 (491), 1113–1125.

Gao, J., Casas, I., 2008. Specification testing in discretized diffusion models: theory and practice. J. Econom. 147 (1), 131–140.

Gao, J., King, M., 2004. Adaptive testing in continuous-time diffusion models. Econom. Theory 20 (5), 844–882.

García-Portugués, E., Álvarez-Liébana, J., 2019. goffda: Goodness-of-fit tests for functional data. R package version 0.0.5.

García-Portugués, E., González-Manteiga, W., Febrero-Bande, M., 2014. A goodness-of-fit test for the functional linear model with scalar response. J. Comput. Graph. Stat. 23 (3), 761–778.

García-Portugués, E., Álvarez-Liébana, J., Álvarez-Pérez, G., González-Manteiga, W., 2021. A goodness-of-fit test for the functional linear model with functional response. Scand. J. Stat. 48 (2), 502–528.

Gelfand, I.M., Vilenkin, N.Y., 1964. Generalized Functions. Academic Press, New York.

González-Manteiga, W., Crujeiras, R.M., 2013. An updated review of goodness-of-fit tests for regression models. Test 22 (3), 361–411.

Hlávka, Z., Hušková, M., Meintanis, S.G., 2021. Testing serial independence with functional data. Test 30 (3), 603–629.

Hong, Y., Li, H., 2004. Nonparametric specification testing for continuous-time models with applications to term structure of interest rates. Rev. Financ. Stud. 18 (1), 37–84.

Hörmann, S., Kokoszka, P., 2010. Weakly dependent functional data. Ann. Stat. 38 (3), 1845–1884.

Horváth, L., Kokoszka, P., 2012. Inference for Functional Data with Applications. Springer Series in Statistics. Springer, New York.

Horváth, L., Husková, M., Kokoszka, P., 2010. Testing the stability of the functional autoregressive process. J. Multivar. Anal. 101 (2), 352–367.

Horváth, L., Kokoszka, P., Rice, G., 2014. Testing stationarity of functional time series. J. Econom. 179, 66–82.

Hörmann, S., Kidzinski, L., Hallin, M., 2015. Dynamic functional principal components. J. R. Stat. Soc. B 77 (2), 319–348.

Karatzas, I., Shreve, S., 1998. Brownian Motion and Stochastic Calculus. Graduate Texts in Mathematics. Springer, New York.

Kim, M., Kokoszka, P., Rice, G., 2023. White noise testing for functional time series. Stat. Surv. 17, 119–168.

Kim, M., Kokoszka, P., Rice, G., 2024. Projection-based white noise and goodness-of-fit tests for functional time series. Stat. Inference Stoch. Process.

Kokoszka, P., Reimherr, M., 2013. Determining the order of the functional autoregressive model. J. Time Ser. Anal. 34 (1), 116–129.

Kokoszka, P., Rice, G., Shang, H.L., 2017. Inference for the autocovariance of a functional time series under conditional heteroscedasticity. J. Multivar. Anal. 162, 32–50.

Koul, H., Stute, W., 1999. Nonparametric model checks for time series. Ann. Stat. 27 (1), 204–236.

Laukaitis, A., Rackauskas, A., 2002. Functional Data Analysis of payment systems. Nonlinear Anal., Model. Control 7, 53–68.

Miller, R.G., 1981. Simultaneous Statistical Inference. Springer-Verlag, New York.

Monsalve-Cobis, A., González-Manteiga, W., Febrero-Bande, M., 2011. Goodness-of-Fit test for interest rate models: an approach based on empirical processes. Comput. Stat. Data Anal. 55 (12), 3073–3092.

Müller, H.G., Sen, R., Stadtmüller, U., 2011. Functional data analysis for volatility. J. Econom. 165 (2), 233–245.

Negri, I., Nishiyama, Y., 2009. Goodness of fit test for ergodic diffusion processes. Ann. Inst. Stat. Math. 61 (4), 919–928.

Podolskij, M., Ziggel, D., 2008. A range-based test for the parametric form of the volatility in diffusion models. CREATES Research Paper, 22.

Rice, G., Wirjanto, T., Zhao, Y., 2020. Tests for conditional heteroscedasticity of functional data. J. Time Ser. Anal. 41, 733–758.

Ruiz-Medina, M.D., Álvarez-Liébana, J., 2019. Classical and Bayesian componentwise predictors for non-compact correlated ARH(1) processes. REVSTAT 17 (3), 265–296.
Ruiz-Medina, M.D., Salmerón, R., 2010. Functional maximum likelihood estimation of ARH(p) models. Stoch. Environ. Res. Risk Assess. 24, 131–146.
Salmerón, R., Ruiz-Medina, M.D., 2009. Multispectral decomposition of functional autoregressive models. Stoch. Environ. Res. Risk Assess. 23, 289–297.
Shang, H.L., 2014. A survey of functional principal component analysis. AStA Adv. Stat. Anal. 98, 121–142.
Shang, H.L., 2018. Bootstrap methods for stationary functional time series. Stat. Comput. 28, 1–10.
Shen, Q., Faraway, J., 2004. An F test for linear models with functional responses. Stat. Sin. 14, 1239–1257.
Song, Z., 2011. A martingale approach for testing diffusion models based on infinitesimal operator. J. Econom. 162 (2), 189–212.
Stute, W., 1997. Nonparametric model checks for regression. Ann. Stat. 25 (2), 613–641.
Uhlenbeck, G.E., Ornstein, L.S., 1930. On the theory of the Brownian motion. Phys. Rev. 36 (5), 823.
Vasicek, O., 1977. An equilibrium characterization of the term structure. J. Financ. Econ. 5 (2), 177–188.
Vieu, P., 2018. On dimension reduction models for functional data. Stat. Probab. Lett. 136, 134–138.
Yao, F., Müller, H.G., Wang, J., 2005. Functional Data Analysis for sparse longitudinal data. J. Am. Stat. Assoc. 100 (470), 577–590.
Yeh, C.K., Rice, G., Dubin, J.A., 2023. Functional spherical autocorrelation: a robust estimate of the autocorrelation of a functional time series. Electron. J. Stat. 17, 650–687.
Zhang, X., 2016. White noise testing and model diagnostic checking for functional time series. J. Econom. 194 (1), 76–95.
Zheng, Z., 2009. Testing heteroscedasticity in nonlinear and nonparametric regressions. Can. J. Stat. 37 (2), 282–300.